

Clustering Functional Data via Variational Inference

Chengqian Xian^{1*}, Camila P. E. de Souza¹, John Jewell², and Ronaldo Dias³

¹Department of Statistical and Actuarial Sciences, University of Western Ontario

²Department of Computer Science, University of Western Ontario

³Department of Statistics, University of Campinas

*Correspondence: cxian3@uwo.ca

Abstract

Functional data analysis deals with data recorded densely over time (or any other continuum) with one or more observed curves per subject. Conceptually, functional data are continuously defined, but in practice, they are usually observed at discrete points. Among different kinds of functional data analyses, clustering analysis aims to determine underlying groups of curves in the dataset when there is no information on the group membership of each individual curve. In this work, we propose a new model-based approach for clustering and smoothing functional data simultaneously via variational inference. We derive coordinate ascent mean-field variational Bayes algorithms to approximate the posterior distribution of our model parameters by finding the variational distribution with the smallest Kullback-Leibler divergence to the posterior. Performance of our proposed method is evaluated using simulated data and publicly available datasets.

Keywords: Functional data analysis, Model-based clustering, Bayesian variational inference

1 Introduction

Functional data analysis (FDA), term first coined by Ramsay and Dalzell (1991), deals with the analysis of data that are defined on some continuum such as time. Theoretically, data are in the form of functions, but in practice they are observed as a series of discrete points representing an underlying curve. Ramsay and Silverman (2005) establish a foundation for FDA on topics including smoothing functional data, functional principal components analysis and functional linear models. Ramsay et al. (2009) provide a guide for analyzing functional data in R and Matlab using publicly available datasets. A comprehensive review of FDA is provided by Wang et al. (2016), in which clustering and classification methods for functional data are also discussed. Functional data analysis has been applied to various research areas such as energy consumption (Lenzi et al., 2017; De Souza et al., 2017; Franco et al., 2021), rainfall data visualization (Hael et al., 2020), income distribution (Hu et al., 2021), spectroscopy (Dias et al., 2015; Yang et al., 2021; Frizzarin et al., 2021), and Covid-19 pandemic (Boschi et al., 2021), among others.

Cluster analysis of functional data aims to determine underlying groups in a set of observed curves when there is no information on the group label of each curve. As described in Jacques and Preda (2014), there are three main types of methods used for functional data clustering: dimension reduction-based (or filtering) methods, distance-based methods, and model-based methods. Functional data generally belongs to the infinite-dimensional space, making those clustering methods for finite-dimensional data ineffective. Dimension reduction-based methods have been proposed to solve this problem. Before clustering, a dimension reduction step (also called *filtering* in James and Sugar, 2003) is carried out by the techniques including spline basis function expansion (Tarpey and Kinader, 2003) and functional principal component analysis (FPCA) (Jones and Rice, 1992). Clustering is then performed using the basis expansion coefficients or the principal component scores, resulting in a two-stage clustering procedure. Distance-based methods are the most well-known and most popular approach for clustering functional data since no parametric assumptions are needed for these algorithms. Nonparametric clustering techniques, including k-means clustering (Hartigan and Wong, 1979) and hierarchical clustering (Ward, 1963), are usually applied using specific distances or dissimilarities between curves (Delaigle et al., 2019; Martino et al., 2019; Li and Ma, 2020). It is important to note that distance-based methods are sometimes equivalent to dimension reduction-based methods if, for example, distance is computed using the basis expansion coefficients. Another widely-used approach is model-based clustering, where functional data are assumed to arise from a mixture of underlying probability distributions. For example,

in Bayesian hierarchical clustering, a common methodology is to assume that the set of coefficients in the basis expansion representing functional data follow a mixture of Gaussian distributions (Wang et al., 2016). To our knowledge, inference in model-based clustering for functional data is generally motivated by the Expectation-Maximization (EM) algorithm (Samé et al., 2011; Jacques and Preda, 2013; Giacomini et al., 2013; Chamroukhi, 2016) or Markov Chain Monte Carlo (MCMC) sampling techniques (Ray and Mallick, 2006).

More recently, Zambom et al. (2019) proposed a method for clustering functional data via hypothesis testing where they replaced the classical distance computation step in the k -means algorithm with hypothesis tests to decide to which cluster a curve belongs. However, these authors first smooth the curves and then apply the test-based clustering procedure, which falls in the scope of two-stage clustering.

In this paper, we propose a new model-based approach for clustering functional data via Bayesian variational inference. We model the raw data obtaining clustering assignments and cluster-specific smooth mean curves simultaneously. To our knowledge, this is the first attempt to use variational inference in the context of functional data clustering. Our proposed method is implemented as an R package and available at <https://github.com/jewelltaylor/funclustVI>.

The remainder of the paper is organized as follows. Section 2 presents an overview of variational inference, our model settings and proposed algorithm. In Section 3, we extend the model by adding a random intercept to obtain a more flexible algorithm. In Section 4, we conduct a study to assess the performance of our methods under various scenarios. In Section 5, we apply our model without the random intercept to two different real datasets. A short conclusion of our study and a discussion on the proposed method are provided in Section 6.

2 Methodology

2.1 Overview of Variational Inference

Variational inference (VI) is a method from machine learning that approximates the posterior density in a Bayesian model through optimization (Jordan et al., 1999; Wainwright et al., 2008). Blei et al. (2017) provide an interesting review of VI from a statistical perspective, including some guidance on when to use MCMC or VI. For example, one may apply VI to large datasets and scenarios where the interest is to develop probabilistic models. In contrast, one may apply MCMC to small datasets for more precise

samples but with a higher computational cost. In Bayesian inference, our goal is to find the posterior density, denoted by $p(\cdot|y)$ where y corresponds to the observed data. One can apply Bayes' theorem to find the posterior, but this might not be easy if there are many parameters and non-conjugate prior distributions. Therefore, one can aim to find an approximation to the posterior. To be specific, one wants to find q^* coming from a family of possible densities Q to approximate $p(\cdot|y)$, which can be solved in terms of an optimization problem with criterion f as follows:

$$q^* = \operatorname{argmin}_{q \in Q} f(q(\cdot), p(\cdot|y)).$$

The criterion f measures the closeness between the possible densities q in the family Q and the exact posterior density p . When we consider the Kullback-Leibler (KL) divergence (Kullback and Leibler, 1951) as criterion f , i.e.,

$$q^* = \operatorname{argmin}_{q \in Q} \text{KL}(q(\cdot)||p(\cdot|y)), \quad (1)$$

this optimization-based technique to approximate the posterior density is called Variational Bayes (VB). (Jordan et al., 1999) and Blei et al. (2017) show that minimizing the KL divergence is equivalent to maximizing the so-called evidence lower bound (ELBO). Let θ be a set of latent model variables, the KL divergence is defined as

$$\text{KL}(q(\cdot)||p(\cdot|y)) := \int q(\theta) \log \frac{q(\theta)}{p(\theta|y)} d\theta,$$

and it can be shown that

$$\int q(\theta) \log \frac{q(\theta)}{p(\theta|y)} d\theta = \log p(y) - \int q(\theta) \log \frac{p(\theta, y)}{q(\theta)} d\theta$$

where the last term is the ELBO. Since $\log p(y)$ is a constant with respect to $q(\theta)$, this changes the problem in (1) to

$$q^* = \operatorname{argmax}_{q \in Q} \text{ELBO}(q). \quad (2)$$

We, therefore, derive a VB algorithm for functional data clustering and implement it as an R package. We consider the mean-field variational family in which the latent variables are mutually independent, and a distinct factor governs each of them in the variational density. Finally, we apply the coordinate ascent variational inference (CAVI) algorithm (Bishop, 2006) to solve the optimization problem in (2).

2.2 Assumptions and model settings

Let $\mathbf{Y}_i, i = 1, \dots, N$, denote the observed data from N curves, and for each curve i there are n evaluation points, t_1, \dots, t_n , so that $\mathbf{Y}_i = (Y_i(t_1), \dots, Y_i(t_n))^T$. Let Z_i be a hidden variable taking values in $\{1, \dots, K\}$ that determines which cluster \mathbf{Y}_i belongs to. We assume Z_1, \dots, Z_N are independent and identically distributed with $P(Z_i = k) = \pi_k, k = 1, \dots, K$, and $\sum_{k=1}^K \pi_k = 1$. For each cluster k , there is a smooth function $f_k(\mathbf{t}) = (f_k(t_1), \dots, f_k(t_n))^T$ and we assume that

$$\mathbf{Y}_i | (Z_i = k) = f_k(\mathbf{t}) + \sigma_k \boldsymbol{\epsilon}_i,$$

with independent errors $\boldsymbol{\epsilon}_1, \dots, \boldsymbol{\epsilon}_N$ and $\boldsymbol{\epsilon}_i \sim MVN(\mathbf{0}, \mathbf{I}_n), i = 1, \dots, N$, where \mathbf{I}_n is an identity matrix of size n . The functions f_1, \dots, f_K can be written as a linear combination of M known B-spline basis functions, that is, $f_k(t_j) = \sum_{m=1}^M B_m(t_j) \phi_{km}, j = 1, \dots, n$, so that $f_k(\mathbf{t}) = \mathbf{B}_{(n \times M)} \boldsymbol{\phi}_{k(M \times 1)}, k = 1, \dots, K$. Therefore,

$$\mathbf{Y}_i | Z_i = k \sim MVN(\mathbf{B} \boldsymbol{\phi}_k, \sigma_k^2 \mathbf{I}), i = 1, \dots, N, k = 1, \dots, K.$$

Let $\mathbf{Z} = (Z_1, \dots, Z_N)^T$, $\boldsymbol{\phi} = \{\boldsymbol{\phi}_1, \dots, \boldsymbol{\phi}_K\}$, $\boldsymbol{\pi} = (\pi_1, \dots, \pi_K)^T$ and $\boldsymbol{\tau} = (\tau_1, \dots, \tau_K)^T$, where $\tau_k = 1/\sigma_k^2$ is the precision parameter. We develop a Bayesian approach to infer $\mathbf{Z}, \boldsymbol{\phi}, \boldsymbol{\pi}$ and $\boldsymbol{\tau}$ via VB; that is, we derive a procedure that, for given data, approximates the posterior distribution by finding the variational distribution (VD), $q(\mathbf{Z}, \boldsymbol{\pi}, \boldsymbol{\phi}, \boldsymbol{\tau})$, with smallest Kullback-Leibler divergence to the posterior distribution $p(\mathbf{Z}, \boldsymbol{\pi}, \boldsymbol{\phi}, \boldsymbol{\tau} | \mathbf{Y})$, which is equivalent to maximizing the evidence lower bound (ELBO) given by

$$\text{ELBO}(q) = \mathbb{E}[\log p(\mathbf{Y}, \mathbf{Z}, \boldsymbol{\pi}, \boldsymbol{\phi}, \boldsymbol{\tau})] - \mathbb{E}[\log q(\mathbf{Z}, \boldsymbol{\pi}, \boldsymbol{\phi}, \boldsymbol{\tau})]. \quad (3)$$

Assuming the following prior distributions for our model parameters:

- $\boldsymbol{\pi} \sim \text{Dirichlet}(\mathbf{d}^0)$;
- $\boldsymbol{\phi}_k \sim MVN(\mathbf{m}_k^0, s^0 \mathbf{I})$ with precision $v^0 = 1/s^0$;
- $\tau_k = 1/\sigma_k^2 \sim \text{Gamma}(a^0, r^0), k = 1, \dots, K$.

2.3 Steps of the VB algorithm

This section describes the main steps of the VB algorithm for inferring $\mathbf{Z}, \boldsymbol{\phi}, \boldsymbol{\pi}$ and $\boldsymbol{\tau}$, which is summarized in Algorithm 1. First, we assume that the variational distribution belongs to the mean-field

variational family, where \mathbf{Z} , $\boldsymbol{\phi}$, $\boldsymbol{\pi}$ and $\boldsymbol{\tau}$ are mutually independent and each governed by a distinct factor in the variational density:

$$q(\mathbf{Z}, \boldsymbol{\pi}, \boldsymbol{\phi}, \boldsymbol{\tau}) = \prod_{i=1}^N q(Z_i) \times \prod_{k=1}^K q(\boldsymbol{\phi}_k) \times \prod_{k=1}^K q(\boldsymbol{\tau}_k) \times q(\boldsymbol{\pi}) \quad (4)$$

We then derive a coordinate ascent algorithm to obtain the VD (Jordan et al., 1999; Blei et al., 2017). That is, we derive an update equation for each term in the factorization (4) by calculating the expectation of $\log p(\mathbf{Y}, \mathbf{Z}, \boldsymbol{\pi}, \boldsymbol{\phi}, \boldsymbol{\tau})$ (the joint distribution of the observed data \mathbf{Y} , hidden variables \mathbf{Z} and parameters $\boldsymbol{\pi}, \boldsymbol{\phi}, \boldsymbol{\tau}$, which is also called complete data log-likelihood) over the VD of all random variables except the one of interest, where

$$\begin{aligned} \log p(\mathbf{Y}, \mathbf{Z}, \boldsymbol{\pi}, \boldsymbol{\phi}, \boldsymbol{\tau}) &= \log p(\mathbf{Y}|\mathbf{Z}, \boldsymbol{\phi}, \boldsymbol{\tau}) + \log p(\mathbf{Z}|\boldsymbol{\pi}) \\ &\quad + \log p(\boldsymbol{\phi}) + \log p(\boldsymbol{\tau}) + \log p(\boldsymbol{\pi}). \end{aligned} \quad (5)$$

So, for example, the optimal update equation for $q(\boldsymbol{\pi})$, $q^*(\boldsymbol{\pi})$, is given by calculating

$$\log q^*(\boldsymbol{\pi}) = \mathbb{E}_{-\boldsymbol{\pi}}(\log p(\mathbf{Y}, \mathbf{Z}, \boldsymbol{\pi}, \boldsymbol{\phi}, \boldsymbol{\tau})) + \text{constant},$$

where $-\boldsymbol{\pi}$ indicates that the expectation is taken with respect to the VD of all other latent variables but $\boldsymbol{\pi}$, i.e., \mathbf{Z} , $\boldsymbol{\phi}$ and $\boldsymbol{\tau}$. In what follows we derive the update equation for each component in our model. For convenience, we use $\overset{+}{\approx}$ to denote equality up to a constant additive factor.

i) Update equation for $q(\boldsymbol{\pi})$

Since only the second term, $\log p(\mathbf{Z}|\boldsymbol{\pi})$, and the last term, $\log p(\boldsymbol{\pi})$, in (5) depend on $\boldsymbol{\pi}$, the update equation $q^*(\boldsymbol{\pi})$ can be derived as follows.

$$\begin{aligned} \log q^*(\boldsymbol{\pi}) &= \mathbb{E}_{-\boldsymbol{\pi}}(\log p(\mathbf{Y}, \mathbf{Z}, \boldsymbol{\pi}, \boldsymbol{\phi}, \boldsymbol{\tau})) \\ &\overset{+}{\approx} \mathbb{E}_{-\boldsymbol{\pi}}(\log p(\mathbf{Z}|\boldsymbol{\pi})) + \mathbb{E}_{-\boldsymbol{\pi}}(\log p(\boldsymbol{\pi})) \\ &= \mathbb{E}_{-\boldsymbol{\pi}}\left[\sum_{i=1}^N \sum_{k=1}^K \mathbf{I}(Z_i = k) \log \pi_k\right] + \log p(\boldsymbol{\pi}) \\ &= \sum_{k=1}^K \log \pi_k \left[\sum_{i=1}^N \mathbb{E}_{q^*(Z_i)}(\mathbf{I}(Z_i = k))\right] + \sum_{k=1}^K [d_k^0 - 1] \log \pi_k \\ &= \sum_{k=1}^K \log \pi_k \left[\left(\sum_{i=1}^N \mathbb{E}_{q^*(Z_i)}(\mathbf{I}(Z_i = k)) + d_k^0\right) - 1\right]. \end{aligned}$$

Therefore, $q^*(\boldsymbol{\pi})$ is a Dirichlet distribution with parameters $\mathbf{d}^* = (d_1^*, \dots, d_K^*)$, where

$$d_k^* = d_k^0 + \sum_{i=1}^N \mathbb{E}_{q^*(Z_i)}(\mathbf{I}(Z_i = k)). \quad (6)$$

ii) *Update equation for $q(Z_i)$*

$$\log q^*(Z_i) \overset{+}{\approx} \mathbb{E}_{-Z_i}(\log p(\mathbf{Y}, \mathbf{Z}, \boldsymbol{\pi}, \boldsymbol{\phi}, \boldsymbol{\tau})) \quad (7)$$

When taking the expectation above we just need to consider the first term, $\log p(\mathbf{Y}|\mathbf{Z}, \boldsymbol{\phi}, \boldsymbol{\tau})$, and the second term, $\log p(\mathbf{Z}|\boldsymbol{\pi})$, in (5). Note that we can write $\log p(\mathbf{Y}|\mathbf{Z}, \boldsymbol{\phi}, \boldsymbol{\tau})$ and $\log p(\mathbf{Z}|\boldsymbol{\pi})$ into two parts, one that depends on Z_i and one that does not.

$$\begin{aligned} \log p(\mathbf{Y}|\mathbf{Z}, \boldsymbol{\phi}, \boldsymbol{\tau}) &= \sum_{k=1}^K \mathbf{I}(Z_i = k) \log p(\mathbf{Y}_i | Z_i = k, \boldsymbol{\phi}_k, \tau_k) \\ &\quad + \sum_{l:l \neq i}^K \sum_{k=1}^K \mathbf{I}(Z_l = k) \log p(\mathbf{Y}_l | Z_l = k, \boldsymbol{\phi}_k, \tau_k) \end{aligned}$$

$$\log p(\mathbf{Z}|\boldsymbol{\pi}) = \sum_{k=1}^K \mathbf{I}(Z_i = k) \log \pi_k + \sum_{l:l \neq i}^K \sum_{k=1}^K \mathbf{I}(Z_l = k) \log \pi_k$$

Now when taking the expectation in (7) the parts that do not depend on Z_i in $\log p(\mathbf{Y}|\mathbf{Z}, \boldsymbol{\phi}, \boldsymbol{\tau})$ and $\log p(\mathbf{Z}|\boldsymbol{\pi})$ in (5) will be added as a constant in the expectation. So, we obtain

$$\begin{aligned} \log q^*(Z_i) &\overset{+}{\approx} \sum_{k=1}^K \mathbf{I}(Z_i = k) \left\{ \frac{n}{2} \mathbb{E}_{q^*(\tau_k)}(\log \tau_k) \right. \\ &\quad \left. - \frac{1}{2} \mathbb{E}_{q^*(\tau_k)}(\tau_k) \mathbb{E}_{q^*(\boldsymbol{\phi}_k)}[(\mathbf{Y}_i - \mathbf{B}\boldsymbol{\phi}_k)^T (\mathbf{Y}_i - \mathbf{B}\boldsymbol{\phi}_k)] \right. \\ &\quad \left. + \mathbb{E}_{q^*(\boldsymbol{\pi})}(\log \pi_k) \right\} \end{aligned}$$

Therefore, $q^*(Z_i)$ is a categorical distribution with parameters

$$p_{ik}^* = \frac{e^{\alpha_{ik}}}{\sum_{k=1}^K e^{\alpha_{ik}}}, \quad (8)$$

where

$$\alpha_{ik} = \frac{n}{2} \mathbb{E}_{q^*(\tau_k)}(\log \tau_k) - \frac{1}{2} \mathbb{E}_{q^*(\tau_k)}(\tau_k) \mathbb{E}_{q^*(\boldsymbol{\phi}_k)}[(\mathbf{Y}_i - \mathbf{B}\boldsymbol{\phi}_k)^T (\mathbf{Y}_i - \mathbf{B}\boldsymbol{\phi}_k)] + \mathbb{E}_{q^*(\boldsymbol{\pi})}(\log \pi_k).$$

iii) Update equation for $q(\boldsymbol{\phi}_k)$

Note that only the first term, $\log p(\mathbf{Y}|\mathbf{Z}, \boldsymbol{\phi}, \boldsymbol{\tau})$, and the third term, $\log p(\boldsymbol{\phi})$, in (5) depend on $\boldsymbol{\phi}_k$. Similarly to the previous case for $q^*(Z_i)$, we can write $\log p(\mathbf{Y}|\mathbf{Z}, \boldsymbol{\phi}, \boldsymbol{\tau})$ and $\log p(\boldsymbol{\phi})$ in two parts, one that depends on $\boldsymbol{\phi}_k$ and the other that does not. Therefore, we obtain

$$\begin{aligned} \log q^*(\boldsymbol{\phi}_k) &\stackrel{+}{\approx} \mathbb{E}_{-\boldsymbol{\phi}_k}(\log p(\mathbf{Y}, \mathbf{Z}, \boldsymbol{\pi}, \boldsymbol{\phi}, \boldsymbol{\tau})) \\ &\stackrel{+}{\approx} \frac{n}{2} \mathbb{E}_{q^*(\tau_k)}(\log \tau_k) \sum_i \mathbb{E}_{q^*(Z_i)}[\mathbb{I}(Z_i = k)] \\ &\quad - \frac{1}{2} \mathbb{E}_{q^*(\tau_k)}(\tau_k) \sum_i \mathbb{E}_{q^*(Z_i)}[\mathbb{I}(Z_i = k)] (\mathbf{Y}_i - \mathbf{B}\boldsymbol{\phi}_k)^T (\mathbf{Y}_i - \mathbf{B}\boldsymbol{\phi}_k) \end{aligned} \quad (9)$$

$$- \frac{M}{2} \log v^0 - \frac{1}{2} v^0 (\boldsymbol{\phi}_k - \mathbf{m}_k^0)^T (\boldsymbol{\phi}_k - \mathbf{m}_k^0) \quad (10)$$

All expectations will be later defined, but note that, for example, $\mathbb{E}_{q^*(Z_i)}[\mathbb{I}(Z_i = k)] = p_{ik}^*$. First, we will focus on the quadratic forms that appear in (9) and (10).

$$\begin{aligned} & - \frac{1}{2} \mathbb{E}_{q^*(\tau_k)}(\tau_k) \sum_i p_{ik}^* (\mathbf{Y}_i - \mathbf{B}\boldsymbol{\phi}_k)^T (\mathbf{Y}_i - \mathbf{B}\boldsymbol{\phi}_k) - \frac{1}{2} v^0 (\boldsymbol{\phi}_k - \mathbf{m}_k^0)^T (\boldsymbol{\phi}_k - \mathbf{m}_k^0) = \\ & - \frac{1}{2} \mathbb{E}_{q^*(\tau_k)}(\tau_k) \sum_i p_{ik}^* [\mathbf{Y}_i^T \mathbf{Y}_i - 2 \mathbf{Y}_i^T \mathbf{B}\boldsymbol{\phi}_k + \boldsymbol{\phi}_k^T \mathbf{B}^T \mathbf{B}\boldsymbol{\phi}_k] \\ & - \frac{1}{2} v^0 [\boldsymbol{\phi}_k^T \boldsymbol{\phi}_k - 2 (\mathbf{m}_k^0)^T \boldsymbol{\phi}_k + (\mathbf{m}_k^0)^T \mathbf{m}_k^0] \stackrel{+}{\approx} \\ & - \frac{1}{2} \boldsymbol{\phi}_k^T \left[v^0 \mathbf{I} + \mathbb{E}_{q^*(\tau_k)}(\tau_k) \sum_i p_{ik}^* \mathbf{B}^T \mathbf{B} \right] \boldsymbol{\phi}_k - \frac{1}{2} (-2) \left[v^0 (\mathbf{m}_k^0)^T + \mathbb{E}_{q^*(\tau_k)}(\tau_k) \sum_i p_{ik}^* \mathbf{Y}_i^T \mathbf{B} \right] \boldsymbol{\phi}_k \end{aligned} \quad (11)$$

Now let

$$\boldsymbol{\Sigma}_k^* = \left[v^0 \mathbf{I} + \mathbb{E}_{q^*(\tau_k)}(\tau_k) \sum_i p_{ik}^* \mathbf{B}^T \mathbf{B} \right]^{-1}. \quad (12)$$

We can then rewrite (11) as

$$- \frac{1}{2} \boldsymbol{\phi}_k^T \boldsymbol{\Sigma}_k^{*-1} \boldsymbol{\phi}_k - \frac{1}{2} (-2) \left[v^0 (\mathbf{m}_k^0)^T + \mathbb{E}_{q^*(\tau_k)}(\tau_k) \sum_i p_{ik}^* \mathbf{Y}_i^T \mathbf{B} \right] \boldsymbol{\Sigma}_k^* \boldsymbol{\Sigma}_k^{*-1} \boldsymbol{\phi}_k.$$

Therefore, $q^*(\boldsymbol{\phi}_k)$ is $MVN(\mathbf{m}_k^*, \boldsymbol{\Sigma}_k^*)$ with $\boldsymbol{\Sigma}_k^*$ as in (12) and mean vector

$$\mathbf{m}_k^* = \left[v^0 (\mathbf{m}_k^0)^T + \mathbb{E}_{q^*(\tau_k)}(\tau_k) \sum_i p_{ik}^* \mathbf{Y}_i^T \mathbf{B} \right] \boldsymbol{\Sigma}_k^*. \quad (13)$$

iv) Update equation for $q(\tau_k)$

Similarly to the calculations in i) and ii) we can write

$$\begin{aligned} \log q^*(\tau_k) &\stackrel{+}{\approx} \frac{n}{2} \log \tau_k \sum_i p_{ik}^* - \frac{1}{2} \tau_k \sum_i p_{ik}^* \mathbb{E}_{q^*(\phi_k)}[(\mathbf{Y}_i - \mathbf{B}\phi_k)^T(\mathbf{Y}_i - \mathbf{B}\phi_k)] \\ &+ (a^0 - 1) \log \tau_k - r^0 \tau_k \end{aligned}$$

Therefore, $q^*(\tau_k)$ is a Gamma distribution with parameters

$$A_k^* = a^0 + \frac{n}{2} \sum_i p_{ik}^* \quad (14)$$

and

$$R_k^* = \left(r^0 + \frac{1}{2} \sum_i p_{ik}^* \mathbb{E}_{q^*(\phi_k)}[(\mathbf{Y}_i - \mathbf{B}\phi_k)^T(\mathbf{Y}_i - \mathbf{B}\phi_k)] \right). \quad (15)$$

Next, we calculate the expectations in the update equations for each component in the VD. Let Ψ be the digamma function defined as

$$\Psi(x) = \frac{d}{dx} \log \Gamma(x), \quad (16)$$

which can be easily calculated via numerical approximation. The values of the expectations taken with respect to the approximated distributions are given as follows.

$$\mathbb{E}_{q^*(Z_i)}[\mathbb{I}(Z_i = k)] = p_{ik}^* \quad (17)$$

$$\mathbb{E}_{q^*(\tau_k)}(\tau_k) = \frac{A_k^*}{R_k^*} \quad (18)$$

$$\mathbb{E}_{q^*(\tau_k)}(\log \tau_k) = \Psi(A_k^*) - \log R_k^* \quad (19)$$

$$\mathbb{E}_{q^*(\boldsymbol{\pi})}(\log \pi_k) = \Psi(d_k^*) - \Psi\left(\sum_{k=1}^K d_k^*\right) \quad (20)$$

In addition, using the fact that $\mathbb{E}(\mathbf{X}^T \mathbf{X}) = \text{trace}[\text{Var}(\mathbf{X})] + \mathbb{E}(\mathbf{X})^T \mathbb{E}(\mathbf{X})$, we obtain

$$\mathbb{E}_{q^*(\phi)}[(\mathbf{Y}_i - \mathbf{B}\phi_k)^T(\mathbf{Y}_i - \mathbf{B}\phi_k)] = \text{trace}(\mathbf{B}\boldsymbol{\Sigma}_k^* \mathbf{B}^T) + (\mathbf{Y}_i - \mathbf{B}\mathbf{m}_k^*)^T(\mathbf{Y}_i - \mathbf{B}\mathbf{m}_k^*). \quad (21)$$

Algorithm 1: Clustering functional data via variational inference

Data: N original curves with n evaluation points; number of clusters K ; values of

hyperparameters: $\mathbf{d}^0, \mathbf{m}_k^0, k = 1, \dots, K, s^0, a^0, r^0$; convergence threshold and maximum number of iterations

Result: VB estimated mean curves for each cluster and the cluster index for each original curve

```
1 Initialization: initialize  $R_k^*$  with arbitrary values (e.g.,  $R_k^* = r^0$ ) and  $p_{ik}^*$  from k-means, and set  
    $c = 0$ ;  
2 while  $c < \text{maximum number of iterations and difference of ELBO} > \text{convergence threshold}$  do  
3   repeat  
4      $c = c + 1$ ;  
5     update  $A_k^{*(c)}$  using  $p_{1k}^{*(c-1)}, \dots, p_{Nk}^{*(c-1)}$  with equation (14);  
6     update  $\Sigma_k^{*(c)}$  using  $A_k^{*(c)}, R_k^{*(c-1)}$  and  $p_{1k}^{*(c-1)}, \dots, p_{Nk}^{*(c-1)}$  with equations (12) and (18);  
7     update  $\mathbf{m}_k^{*(c)}$  using  $\Sigma_k^{*(c)}, A_k^{*(c)}, R_k^{*(c-1)}$  and  $p_{1k}^{*(c-1)}, \dots, p_{Nk}^{*(c-1)}$  with equations (13) and (18);  
8     update  $R_k^{*(c)}$  using  $\mathbf{m}_k^{*(c)}, \Sigma_k^{*(c)}$  and  $p_{1k}^{*(c-1)}, \dots, p_{Nk}^{*(c-1)}$  with equations (15) and (21);  
9     update  $\mathbf{d}^{*(c)}$  using  $p_{1k}^{*(c-1)}, \dots, p_{Nk}^{*(c-1)}$  with equations (6) and (17);  
10    update  $p_{1k}^{*(c)}, \dots, p_{Nk}^{*(c)}$  using  $R_k^{*(c)}, \mathbf{d}^{*(c)}, \mathbf{m}_k^{*(c)}$  and  $\Sigma_k^{*(c)}$  with equations (8), (18), (19), (20)  
      and (21);  
11    calculate the current ELBO,  $\text{ELBO}^{(c)}$  using formulas in section 2.4;  
12    difference of ELBO =  $\text{ELBO}^{(c)} - \text{ELBO}^{(c-1)}$ ;  
13  until maximum iteration is achieved or the ELBO converges;  
14 end
```

2.4 ELBO calculation

In this section, we show how to calculate the ELBO, which is the convergence criterion of our proposed VB algorithm and will be updated at the end of each iteration until it converges. Equation (3) gives the ELBO:

$$\text{ELBO}(q) = \mathbb{E}_{q^*}[\log p(\mathbf{Y}, \mathbf{Z}, \boldsymbol{\pi}, \boldsymbol{\phi}, \boldsymbol{\tau})] - \mathbb{E}_{q^*}[\log q(\mathbf{Z}, \boldsymbol{\pi}, \boldsymbol{\phi}, \boldsymbol{\tau})],$$

where

$$\begin{aligned}\mathbb{E}_{q^*}[\log p(\mathbf{Y}, \mathbf{Z}, \boldsymbol{\pi}, \boldsymbol{\phi}, \boldsymbol{\tau})] &= \mathbb{E}_{q^*}[\log p(\mathbf{Y}|\mathbf{Z}, \boldsymbol{\pi}, \boldsymbol{\phi}, \boldsymbol{\tau})] + \mathbb{E}_{q^*}[\log p(\mathbf{Z}|\boldsymbol{\pi})] + \\ &\quad \mathbb{E}_{q^*}[\log p(\boldsymbol{\phi})] + \mathbb{E}_{q^*}[\log p(\boldsymbol{\tau})] + \mathbb{E}_{q^*}[\log p(\boldsymbol{\pi})],\end{aligned}$$

and

$$\mathbb{E}_{q^*}[\log q(\mathbf{Z}, \boldsymbol{\pi}, \boldsymbol{\phi}, \boldsymbol{\tau})] = \mathbb{E}_{q^*}[\log q(\mathbf{Z})] + \mathbb{E}_{q^*}[\log q(\boldsymbol{\phi})] + \mathbb{E}_{q^*}[\log q(\boldsymbol{\pi})] + \mathbb{E}_{q^*}[\log q(\boldsymbol{\tau})]$$

Therefore, we can write the ELBO as the summation of 5 terms:

$$\text{ELBO}(q) = \mathbb{E}_{q^*}[\log p(\mathbf{Y}|\mathbf{Z}, \boldsymbol{\pi}, \boldsymbol{\phi}, \boldsymbol{\tau})] + \text{diff}_{\mathbf{Z}} + \text{diff}_{\boldsymbol{\phi}} + \text{diff}_{\boldsymbol{\tau}} + \text{diff}_{\boldsymbol{\pi}} \quad (22)$$

where,

$$\text{diff}_{\mathbf{Z}} = \mathbb{E}_{q^*}[\log p(\mathbf{Z}|\boldsymbol{\pi})] - \mathbb{E}_{q^*}[\log q(\mathbf{Z})].$$

Specifically,

$$\text{diff}_{\mathbf{Z}} \equiv \sum_{i=1}^N \sum_{k=1}^K p_{ik}^* \mathbb{E}_{q^*}(\boldsymbol{\pi})(\log \pi_k) - \sum_{i=1}^N \sum_{k=1}^K p_{ik}^* \log p_{ik}^*. \quad (23)$$

The other terms in (22) are calculated as follows:

$$\text{diff}_{\boldsymbol{\phi}} \equiv -\frac{1}{2} \sum_{k=1}^K v_k^0 \{\text{trace}(\boldsymbol{\Sigma}_k^*) + (\mathbf{m}_k^* - \mathbf{m}_k^0)^T (\mathbf{m}_k^* - \mathbf{m}_k^0)\} + \frac{1}{2} \sum_{k=1}^K \log |\boldsymbol{\Sigma}_k^*|,$$

$$\text{diff}_{\boldsymbol{\tau}} \equiv \sum_{k=1}^K \{(a^0 - 1) \mathbb{E}_{q^*(\tau_k)}(\log \tau_k) - r^0 \mathbb{E}_{q^*(\tau_k)}(\tau_k)\} - \sum_{k=1}^K \{A_k^* \log R_k^* + (A_k^* - 1) \mathbb{E}_{q^*(\tau_k)}(\log \tau_k)\},$$

$$\text{diff}_{\boldsymbol{\pi}} \equiv \sum_{k=1}^K (d_k^0 - d_k^*) \mathbb{E}_{q^*}(\boldsymbol{\pi})(\log \pi_k),$$

and

$$\mathbb{E}_{q^*}[\log p(\mathbf{Y}|\mathbf{Z}, \boldsymbol{\pi}, \boldsymbol{\phi}, \boldsymbol{\tau})] = \sum_{i=1}^N \sum_{k=1}^K p_{ik}^* \left\{ \frac{n}{2} \mathbb{E}_{q^*(\tau_k)}(\log \tau_k) - \frac{1}{2} \frac{A_k^*}{R_k^*} \mathbb{E}_{q^*(\phi)} \left[(\mathbf{Y}_i - \mathbf{B}\boldsymbol{\phi}_k)^T (\mathbf{Y}_i - \mathbf{B}\boldsymbol{\phi}_k) \right] \right\}.$$

Therefore, at iteration c , we calculate $\text{ELBO}^{(c)}$ using all parameters obtained at the end of iteration c . Convergence of the algorithm is achieved if $\text{ELBO}^{(c)} - \text{ELBO}^{(c-1)}$ is smaller than a given threshold. It is important to note that we use the fact that $\lim_{p_{ik}^* \rightarrow 0} p_{ik}^* \log p_{ik}^* = 0$ to avoid numerical issues when calculating (23).

3 An extension

3.1 Assumptions and model settings

We extend the model in Section 2 by adding a random intercept $a_i, i = 1, 2, \dots, N$, to each curve which induces correlation among observations within each curve. The model now becomes:

$$Y_{ij} | (Z_i = k) = a_i + f_k(t_j) + \sigma_k \epsilon_{ij}$$

where $\epsilon_{ij} \sim N(0, 1)$ and $a_i \sim N(0, \sigma_a^2)$. We can write this model in vector form as,

$$\mathbf{Y}_i | (Z_i = k) = a_i \mathbf{1}_n + f_k(\mathbf{t}) + \sigma_k \boldsymbol{\epsilon}_i, i = 1, 2, \dots, N,$$

where $\mathbf{1}_n$ is a vector of length n with all elements equal to 1, and further assume that $\boldsymbol{\epsilon}_i \sim MVN(\mathbf{0}, \mathbf{I}_{n \times n})$ and $a_i \sim N(0, \sigma_a^2)$.

This model can be rewritten as a two-step model:

$$\mathbf{Y}_i | (Z_i = k, a_i) \sim MVN(\mathbf{B}\boldsymbol{\phi}_k + a_i \mathbf{1}_n, \sigma_k^2 \mathbf{I})$$

and $a_i \sim N(0, \sigma_a^2), i = 1, 2, \dots, N$.

In this model, all parameters are $\mathbf{Z} = (Z_1, \dots, Z_N)^T$, $\boldsymbol{\phi} = \{\boldsymbol{\phi}_1, \dots, \boldsymbol{\phi}_K\}$, $\boldsymbol{\pi} = (\pi_1, \dots, \pi_K)^T$, $\boldsymbol{\tau} = (\tau_1, \dots, \tau_K)^T$ with $\tau_k = 1/\sigma_k^2$ and $\mathbf{a} = (a_1, \dots, a_N)^T$ with $\tau_a = 1/\sigma_a^2$.

Assuming the following prior distributions for our model parameters:

- $\boldsymbol{\pi} \sim \text{Dirichlet}(\mathbf{d}^0)$;
- $\boldsymbol{\phi}_k \sim MVN(\mathbf{m}_k^0, s^0 \mathbf{I})$ with precision $v^0 = 1/s^0$;
- $\tau_k = 1/\sigma_k^2 \sim \text{Gamma}(b^0, r^0)$, $k = 1, \dots, K$;
- $\tau_a = 1/\sigma_a^2 \sim \text{Gamma}(\alpha^0, \beta^0)$;
- $a_i \sim N(0, \sigma_a^2)$ with $\tau_a = 1/\sigma_a^2$.

3.2 Algorithm

We present the main steps of the algorithm for the extended model, which is summarized in Algorithm 2.

1. VD factorization:

$$q(\mathbf{Z}, \boldsymbol{\pi}, \boldsymbol{\phi}, \boldsymbol{\tau}, \mathbf{a}, \tau_a) = \prod_{i=1}^N q(Z_i) \times \prod_{k=1}^K q(\boldsymbol{\phi}_k) \times \prod_{k=1}^K q(\tau_k) \times q(\boldsymbol{\pi}) \times \prod_{i=1}^N q(a_i) \times q(\tau_a) \quad (24)$$

2. Complete data log-likelihood:

$$\begin{aligned} \log p(\mathbf{Y}, \mathbf{Z}, \boldsymbol{\pi}, \boldsymbol{\phi}, \boldsymbol{\tau}, \mathbf{a}, \tau_a) &= \log p(\mathbf{Y}|\mathbf{Z}, \boldsymbol{\phi}, \boldsymbol{\tau}, \mathbf{a}) + \log p(\mathbf{Z}|\boldsymbol{\pi}) + \log p(\boldsymbol{\phi}) + \\ &\quad \log p(\boldsymbol{\tau}) + \log p(\boldsymbol{\pi}) + \log p(\mathbf{a}|\tau_a) + \log p(\tau_a). \end{aligned} \quad (25)$$

3. Update equations:

i) Update equation for $q(\boldsymbol{\pi})$

Since only the second term, $\log p(\mathbf{Z}|\boldsymbol{\pi})$, and the fifth term, $\log p(\boldsymbol{\pi})$, in (25) depend on $\boldsymbol{\pi}$, the update equation $q^*(\boldsymbol{\pi})$ can be derived as follows.

$$\begin{aligned} \log q^*(\boldsymbol{\pi}) &= \mathbb{E}_{-\boldsymbol{\pi}}(\log p(\mathbf{Y}, \mathbf{Z}, \boldsymbol{\pi}, \boldsymbol{\phi}, \boldsymbol{\tau}, \mathbf{a}, \tau_a)) \\ &\stackrel{+}{\approx} \mathbb{E}_{-\boldsymbol{\pi}}(\log p(\mathbf{Z}|\boldsymbol{\pi})) + \mathbb{E}_{-\boldsymbol{\pi}}(\log p(\boldsymbol{\pi})) \\ &= \mathbb{E}_{-\boldsymbol{\pi}}\left[\sum_{i=1}^N \sum_{k=1}^K \mathbf{I}(Z_i = k) \log \pi_k\right] + \log p(\boldsymbol{\pi}) \\ &= \sum_{k=1}^K \log \pi_k \left[\sum_{i=1}^N \mathbb{E}_{q^*(Z_i)}(\mathbf{I}(Z_i = k))\right] + \sum_{k=1}^K [d_k^0 - 1] \log \pi_k \\ &= \sum_{k=1}^K \log \pi_k \left[\left(\sum_{i=1}^N \mathbb{E}_{q^*(Z_i)}(\mathbf{I}(Z_i = k)) + d_k^0\right) - 1\right]. \end{aligned}$$

Therefore, $q^*(\boldsymbol{\pi})$ is a Dirichlet distribution with parameters $\mathbf{d}^* = (d_1^*, \dots, d_K^*)$, where

$$d_k^* = d_k^0 + \sum_{i=1}^N \mathbb{E}_{q^*(Z_i)}(\mathbf{I}(Z_i = k)). \quad (26)$$

ii) Update equation for $q(Z_i)$

$$\log q^*(Z_i) = \mathbb{E}_{-Z_i}(\log p(\mathbf{Y}, \mathbf{Z}, \boldsymbol{\pi}, \boldsymbol{\phi}, \boldsymbol{\tau}, \mathbf{a}, \tau_a)) \stackrel{+}{\approx} \mathbb{E}_{-Z_i}(\log p(\mathbf{Y}|\mathbf{Z}, \boldsymbol{\phi}, \boldsymbol{\tau}, \mathbf{a})) + \mathbb{E}_{-Z_i}(\log p(\mathbf{Z}|\boldsymbol{\pi}))$$

Note that

$$\begin{aligned}\log p(\mathbf{Y}, \mathbf{Z}, \boldsymbol{\phi}, \boldsymbol{\tau}, \mathbf{a}) &= \sum_{k=1}^K \mathbf{I}(Z_i = k) \log p(\mathbf{Y}_i | Z_i = k, \boldsymbol{\phi}_k, \tau_k, a_i) \\ &+ \sum_{l:l \neq i} \sum_{k=1}^K \mathbf{I}(Z_l = k) \log p(\mathbf{Y}_l | Z_l = k, \boldsymbol{\phi}_k, \tau_k, a_l)\end{aligned}$$

and

$$\log p(\mathbf{Z} | \boldsymbol{\pi}) = \sum_{k=1}^K \mathbf{I}(Z_i = k) \log \pi_k + \sum_{l:l \neq i} \sum_{k=1}^K \mathbf{I}(Z_l = k) \log \pi_k$$

As a result,

$$\begin{aligned}\log q^*(Z_i) &\overset{+}{\approx} \sum_{k=1}^K \mathbf{I}(Z_i = k) \left\{ \frac{n}{2} \mathbb{E}_{q^*(\tau_k)}(\log \tau_k) \right. \\ &\quad - \frac{1}{2} \mathbb{E}_{q^*(\tau_k)}(\tau_k) \mathbb{E}_{q^*(\boldsymbol{\phi}_k) \cdot q^*(a_i)}[(\mathbf{Y}_i - \mathbf{B}\boldsymbol{\phi}_k - a_i \mathbf{1}_n)^T (\mathbf{Y}_i - \mathbf{B}\boldsymbol{\phi}_k - a_i \mathbf{1}_n)] \\ &\quad \left. + \mathbb{E}_{q^*(\boldsymbol{\pi})}(\log \pi_k) \right\}\end{aligned}$$

Therefore, $q^*(Z_i)$ is a categorical distribution with parameters

$$p_{ik}^* = \frac{e^{\alpha_{ik}}}{\sum_{k=1}^K e^{\alpha_{ik}}}, \quad (27)$$

where

$$\alpha_{ik} = \frac{n}{2} \mathbb{E}_{q^*(\tau_k)}(\log \tau_k) - \frac{1}{2} \mathbb{E}_{q^*(\tau_k)}(\tau_k) \mathbb{E}_{q^*(\boldsymbol{\phi}_k) \cdot q^*(a_i)}[(\mathbf{Y}_i - \mathbf{B}\boldsymbol{\phi}_k - a_i \mathbf{1}_n)^T (\mathbf{Y}_i - \mathbf{B}\boldsymbol{\phi}_k - a_i \mathbf{1}_n)] + \mathbb{E}_{q^*(\boldsymbol{\pi})}(\log \pi_k).$$

iii) Update equation for $q(\boldsymbol{\phi}_k)$

$$\begin{aligned}\log q^*(\boldsymbol{\phi}_k) &\overset{+}{\approx} \mathbb{E}_{-\boldsymbol{\phi}_k}(\log p(\mathbf{Y}, \mathbf{Z}, \boldsymbol{\pi}, \boldsymbol{\phi}, \boldsymbol{\tau}, \mathbf{a}, \tau_a)) \\ &\overset{+}{\approx} \frac{n}{2} \mathbb{E}_{q^*(\tau_k)}(\log \tau_k) \sum_{i=1}^N \mathbb{E}_{q^*(Z_i)}[\mathbf{I}(Z_i = k)] \\ &\quad - \frac{1}{2} \mathbb{E}_{q^*(\tau_k)}(\tau_k) \sum_{i=1}^N \mathbb{E}_{q^*(Z_i)}[\mathbf{I}(Z_i = k)] \mathbb{E}_{q^*(a_i)}[(\mathbf{Y}_i - \mathbf{B}\boldsymbol{\phi}_k - a_i \mathbf{1}_n)^T (\mathbf{Y}_i - \mathbf{B}\boldsymbol{\phi}_k - a_i \mathbf{1}_n)] \\ &\quad + \frac{M}{2} \log v^0 - \frac{1}{2} v^0 (\boldsymbol{\phi}_k - \mathbf{m}_k^0)^T (\boldsymbol{\phi}_k - \mathbf{m}_k^0)\end{aligned}$$

First, note that

$$\mathbb{E}_{q^*(a_i)}[(\mathbf{Y}_i - \mathbf{B}\boldsymbol{\phi}_k - a_i \mathbf{1}_n)^T (\mathbf{Y}_i - \mathbf{B}\boldsymbol{\phi}_k - a_i \mathbf{1}_n)] \overset{+}{\approx} (\mathbf{Y}_i - \mathbf{B}\boldsymbol{\phi}_k - \mu_{a_i}^* \mathbf{1}_n)^T (\mathbf{Y}_i - \mathbf{B}\boldsymbol{\phi}_k - \mu_{a_i}^* \mathbf{1}_n)$$

where $\mu_{a_i}^*$ is the posterior mean of $q^*(a_i)$ which will be derived later.

Therefore, let $\mathbf{Y}_i^* = \mathbf{Y}_i - \mu_{a_i}^* \mathbf{1}_n$, and we have

$$\mathbb{E}_{q^*(a_i)}[(\mathbf{Y}_i - \mathbf{B}\boldsymbol{\phi}_k - a_i \mathbf{1}_n)^T (\mathbf{Y}_i - \mathbf{B}\boldsymbol{\phi}_k - a_i \mathbf{1}_n)] \stackrel{+}{\approx} (\mathbf{Y}_i^* - \mathbf{B}\boldsymbol{\phi}_k)^T (\mathbf{Y}_i^* - \mathbf{B}\boldsymbol{\phi}_k).$$

As a result,

$$\log q^*(\boldsymbol{\phi}_k) \stackrel{+}{\approx} -\frac{1}{2} \boldsymbol{\phi}_k^T \left[v^0 \mathbf{I} + \mathbb{E}_{q^*(\tau_k)}(\tau_k) \sum_{i=1}^N p_{ik}^* \mathbf{B}^T \mathbf{B} \right] \boldsymbol{\phi}_k - \frac{1}{2} (-2) \left[v^0 (\mathbf{m}_k^0)^T + \mathbb{E}_{q^*(\tau_k)}(\tau_k) \sum_{i=1}^N p_{ik}^* \mathbf{Y}_i^{*T} \mathbf{B} \right] \boldsymbol{\phi}_k$$

Let

$$\boldsymbol{\Sigma}_k^* = \left[v^0 \mathbf{I} + \mathbb{E}_{q^*(\tau_k)}(\tau_k) \sum_{i=1}^N p_{ik}^* \mathbf{B}^T \mathbf{B} \right]^{-1}, \quad (28)$$

and

$$\mathbf{m}_k^* = \left[v^0 (\mathbf{m}_k^0)^T + \mathbb{E}_{q^*(\tau_k)}(\tau_k) \sum_{i=1}^N p_{ik}^* \mathbf{Y}_i^{*T} \mathbf{B} \right] \boldsymbol{\Sigma}_k^*, \quad (29)$$

Then $q^*(\boldsymbol{\phi}_k)$ is $MVN(\mathbf{m}_k^*, \boldsymbol{\Sigma}_k^*)$.

iv) *Update equation for $q(\tau_k)$*

$$\begin{aligned} \log q^*(\tau_k) &\stackrel{+}{\approx} \frac{n}{2} \log \tau_k \sum_i p_{ik}^* - \frac{1}{2} \tau_k \sum_i p_{ik}^* \mathbb{E}_{q^*(\boldsymbol{\phi}_k) \cdot q^*(a_i)} [(\mathbf{Y}_i - \mathbf{B}\boldsymbol{\phi}_k - a_i \mathbf{1}_n)^T (\mathbf{Y}_i - \mathbf{B}\boldsymbol{\phi}_k - a_i \mathbf{1}_n)] \\ &+ (b^0 - 1) \log \tau_k - r^0 \tau_k \end{aligned}$$

Therefore, $q^*(\tau_k)$ is a Gamma distribution with parameters

$$A_k^* = b^0 + \frac{n}{2} \sum_i p_{ik}^* \quad (30)$$

and

$$R_k^* = \left(r^0 + \frac{1}{2} \sum_i p_{ik}^* \mathbb{E}_{q^*(\boldsymbol{\phi}_k) \cdot q^*(a_i)} [(\mathbf{Y}_i - \mathbf{B}\boldsymbol{\phi}_k - a_i \mathbf{1}_n)^T (\mathbf{Y}_i - \mathbf{B}\boldsymbol{\phi}_k - a_i \mathbf{1}_n)] \right). \quad (31)$$

v) Update equation for $q(a_i)$

$$\begin{aligned}
\log q^*(a_i) &= \mathbb{E}_{-a_i}(\log p(\mathbf{Y}, \mathbf{Z}, \boldsymbol{\pi}, \boldsymbol{\phi}, \boldsymbol{\tau}, \mathbf{a}, \tau_a)) \\
&\stackrel{+}{\approx} \mathbb{E}_{-a_i}(\log p(\mathbf{Y}|\mathbf{Z}, \boldsymbol{\phi}, \boldsymbol{\tau}, \mathbf{a})) + \mathbb{E}_{-a_i}(\log p(\mathbf{a}|\tau_a)) \\
&\stackrel{+}{\approx} \mathbb{E}_{-a_i} \left[\sum_{k=1}^K \mathbf{I}(Z_i = k) \log p(\mathbf{Y}_i|Z_i = k, \boldsymbol{\phi}_k, \tau_k, a_i) \right] + \mathbb{E}_{-a_i} \left[\sum_{k=1}^K \mathbf{I}(Z_i = k) \log p(a_i|\tau_a) \right] \\
&\stackrel{+}{\approx} \sum_{k=1}^K p_{ik}^* \left\{ \frac{n}{2} \mathbb{E}_{q^*(\tau_k)} \log \tau_k - \frac{1}{2} \mathbb{E}_{q^*(\tau_k)} \tau_k \mathbb{E}_{q^*(\boldsymbol{\phi}_k)} [(\mathbf{Y}_i - \mathbf{B}\boldsymbol{\phi}_k - a_i \mathbf{1}_n)^T (\mathbf{Y}_i - \mathbf{B}\boldsymbol{\phi}_k - a_i \mathbf{1}_n)] - \frac{1}{2} a_i^2 \mathbb{E}_{q^*(\tau_a)} \tau_a \right\} \\
&\stackrel{+}{\approx} \sum_{k=1}^K p_{ik}^* \left\{ -\frac{1}{2} \mathbb{E}_{q^*(\tau_k)} \tau_k [(\mathbf{Y}_i - \mathbf{B}\mathbf{m}_k^* - a_i \mathbf{1}_n)^T (\mathbf{Y}_i - \mathbf{B}\mathbf{m}_k^* - a_i \mathbf{1}_n)] - \frac{1}{2} a_i^2 \mathbb{E}_{q^*(\tau_a)} \tau_a \right\}
\end{aligned}$$

Let $\mathbf{Y}_{ik}^* = \mathbf{Y}_i - \mathbf{B}\mathbf{m}_k^*$, then

$$\begin{aligned}
\log q^*(a_i) &\stackrel{+}{\approx} \sum_{k=1}^K p_{ik}^* \left\{ -\frac{1}{2} \mathbb{E}_{q^*(\tau_k)} \tau_k [(\mathbf{Y}_{ik}^* - a_i \mathbf{1}_n)^T (\mathbf{Y}_{ik}^* - a_i \mathbf{1}_n)] - \frac{1}{2} a_i^2 \mathbb{E}_{q^*(\tau_a)} \tau_a \right\} \\
&\stackrel{+}{\approx} -\frac{n}{2} a_i^2 \sum_{k=1}^K p_{ik}^* \mathbb{E}_{q^*(\tau_k)} \tau_k + a_i \sum_{k=1}^K p_{ik}^* \mathbb{E}_{q^*(\tau_k)} \tau_k \mathbf{1}_n^T \mathbf{Y}_{ik}^* - \frac{1}{2} a_i^2 \mathbb{E}_{q^*(\tau_a)} \tau_a \\
&= -\frac{1}{2} a_i^2 \left[n \sum_{k=1}^K p_{ik}^* \mathbb{E}_{q^*(\tau_k)} \tau_k + \mathbb{E}_{q^*(\tau_a)} \tau_a \right] + a_i \sum_{k=1}^K p_{ik}^* \mathbb{E}_{q^*(\tau_k)} \tau_k \mathbf{1}_n^T \mathbf{Y}_{ik}^*
\end{aligned}$$

Let

$$\sigma_{a_i}^{2*} = \left(n \sum_{k=1}^K p_{ik}^* \mathbb{E}_{q^*(\tau_k)} \tau_k + \mathbb{E}_{q^*(\tau_a)} \tau_a \right)^{-1} \quad (32)$$

and

$$\mu_{a_i}^* = \sigma_{a_i}^{2*} \sum_{k=1}^K p_{ik}^* \mathbb{E}_{q^*(\tau_k)} \tau_k \mathbf{1}_n^T \mathbf{Y}_{ik}^* \quad (33)$$

Then $q^*(a_i)$ is $N(\mu_{a_i}^*, \sigma_{a_i}^{*2})$.

vi) Update equation for $q(\tau_a)$

$$\begin{aligned}
\log q^*(\tau_a) &\stackrel{+}{\approx} \mathbb{E}_{-\tau_a}(\log p(\mathbf{a}|\tau_a) + \log p(\tau_a)) \\
&\stackrel{+}{\approx} \mathbb{E}_{-\tau_a} \left(\sum_{i=1}^N \log p(a_i|\tau_a) \right) + (\alpha^0 - 1) \log \tau_a - \beta^0 \tau_a \\
&\stackrel{+}{\approx} \frac{N}{2} \log \tau_a - \frac{1}{2} \tau_a \sum_{i=1}^N \mathbb{E}_{q^*(a_i)} a_i^2 + (\alpha^0 - 1) \log \tau_a - \beta^0 \tau_a \\
&= \left(\alpha^0 + \frac{N}{2} - 1 \right) \log \tau_a - \left(\beta^0 + \frac{1}{2} \sum_{i=1}^N \mathbb{E}_{q^*(a_i)} a_i^2 \right) \tau_a
\end{aligned}$$

Let

$$\alpha^* = \alpha^0 + \frac{N}{2}$$

and

$$\beta^* = \beta^0 + \frac{1}{2} \sum_{i=1}^N \mathbb{E}_{q^*(a_i)} a_i^2 \quad (34)$$

$q^*(\tau_a)$ is $\text{Gamma}(\alpha^*, \beta^*)$.

4. Expectations:

Next, we calculate the expectations in the update equations for each component in the VD. Let Ψ be the digamma function defined as

$$\Psi(x) = \frac{d}{dx} \log \Gamma(x), \quad (35)$$

which can be easily calculated via numerical approximation. The values of the expectations taken with respect to the approximated distributions are given as follows.

$$\mathbb{E}_{q^*(Z_i)}[\mathbb{I}(Z_i = k)] = p_{ik}^* \quad (36)$$

$$\mathbb{E}_{q^*(\tau_k)}(\tau_k) = \frac{A_k^*}{R_k^*} \quad (37)$$

$$\mathbb{E}_{q^*(\tau_k)}(\log \tau_k) = \Psi(A_k^*) - \log R_k^* \quad (38)$$

$$\mathbb{E}_{q^*(\boldsymbol{\pi})}(\log \pi_k) = \Psi(d_k^*) - \Psi\left(\sum_{k=1}^K d_k^*\right) \quad (39)$$

$$\mathbb{E}_{q^*(\tau_a)}(\tau_a) = \frac{\alpha^*}{\beta^*} \quad (40)$$

$$\mathbb{E}_{q^*(\tau_a)}(\log \tau_a) = \Psi(\alpha^*) - \log \beta^* \quad (41)$$

$$\mathbb{E}_{q^*(a_i)} a_i^2 = \sigma_{a_i}^{*2} + \mu_{a_i}^{*2} \quad (42)$$

In addition, using the fact that $\mathbb{E}(\mathbf{X}^T \mathbf{X}) = \text{trace}[\text{Var}(\mathbf{X})] + \mathbb{E}(\mathbf{X})^T \mathbb{E}(\mathbf{X})$, we obtain

$$\begin{aligned} \mathbb{E}_{q^*(\boldsymbol{\phi}_k)}[(\mathbf{Y}_i - \mathbf{B}\boldsymbol{\phi}_k - a_i \mathbf{1}_n)^T (\mathbf{Y}_i - \mathbf{B}\boldsymbol{\phi}_k - a_i \mathbf{1}_n)] &= \text{trace}(\mathbf{B}\boldsymbol{\Sigma}_k^* \mathbf{B}^T) \\ &+ (\mathbf{Y}_i - \mathbf{B}\mathbf{m}_k^* - a_i \mathbf{1}_n)^T (\mathbf{Y}_i - \mathbf{B}\mathbf{m}_k^* - a_i \mathbf{1}_n), \end{aligned} \quad (43)$$

and

$$\begin{aligned} &\mathbb{E}_{q^*(\boldsymbol{\phi}_k), q^*(a_i)}[(\mathbf{Y}_i - \mathbf{B}\boldsymbol{\phi}_k - a_i \mathbf{1}_n)^T (\mathbf{Y}_i - \mathbf{B}\boldsymbol{\phi}_k - a_i \mathbf{1}_n)] \\ &= \mathbb{E}_{q^*(a_i)}\left[\mathbb{E}_{q^*(\boldsymbol{\phi}_k)}[(\mathbf{Y}_i - \mathbf{B}\boldsymbol{\phi}_k - a_i \mathbf{1}_n)^T (\mathbf{Y}_i - \mathbf{B}\boldsymbol{\phi}_k - a_i \mathbf{1}_n)]\right] \\ &= \mathbb{E}_{q^*(a_i)}\left[\text{trace}(\mathbf{B}\boldsymbol{\Sigma}_k^* \mathbf{B}^T) + (\mathbf{Y}_i - \mathbf{B}\mathbf{m}_k^* - a_i \mathbf{1}_n)^T (\mathbf{Y}_i - \mathbf{B}\mathbf{m}_k^* - a_i \mathbf{1}_n)\right] \\ &= \text{trace}(\mathbf{B}\boldsymbol{\Sigma}_k^* \mathbf{B}^T) + n\sigma_{a_i}^{*2} + (\mathbf{Y}_i - \mathbf{B}\mathbf{m}_k^* - \mu_{a_i}^* \mathbf{1}_n)^T (\mathbf{Y}_i - \mathbf{B}\mathbf{m}_k^* - \mu_{a_i}^* \mathbf{1}_n). \end{aligned} \quad (44)$$

3.3 ELBO calculation

We derive the ELBO calculation in this section. The ELBO is defined as follows in this extended model.

$$\text{ELBO}(q) = \mathbb{E}_{q^*}[\log p(\mathbf{Y}, \mathbf{Z}, \boldsymbol{\pi}, \boldsymbol{\phi}, \boldsymbol{\tau}, \mathbf{a}, \tau_a)] - \mathbb{E}_{q^*}[\log q(\mathbf{Z}, \boldsymbol{\pi}, \boldsymbol{\phi}, \boldsymbol{\tau}, \mathbf{a}, \tau_a)],$$

where

$$\begin{aligned} \mathbb{E}_{q^*}[\log p(\mathbf{Y}, \mathbf{Z}, \boldsymbol{\pi}, \boldsymbol{\phi}, \boldsymbol{\tau}, \mathbf{a}, \tau_a)] &= \mathbb{E}_{q^*}[\log p(\mathbf{Y}|\mathbf{Z}, \boldsymbol{\phi}, \boldsymbol{\tau}, \mathbf{a})] + \mathbb{E}_{q^*}[\log p(\mathbf{Z}|\boldsymbol{\pi})] \\ &+ \mathbb{E}_{q^*}[\log p(\boldsymbol{\phi})] + \mathbb{E}_{q^*}[\log p(\boldsymbol{\tau})] + \mathbb{E}_{q^*}[\log p(\boldsymbol{\phi})] \\ &+ \mathbb{E}_{q^*}[\log p(\mathbf{a}|\tau_a)] + \mathbb{E}_{q^*}[\log p(\tau_a)], \end{aligned}$$

and

$$\begin{aligned} \mathbb{E}_{q^*}[\log q(\mathbf{Z}, \boldsymbol{\pi}, \boldsymbol{\phi}, \boldsymbol{\tau}, \mathbf{a}, \tau_a)] &= \mathbb{E}_{q^*}[\log q(\mathbf{Z})] + \mathbb{E}_{q^*}[\log q(\boldsymbol{\phi})] + \mathbb{E}_{q^*}[\log q(\boldsymbol{\pi})] \\ &+ \mathbb{E}_{q^*}[\log q(\boldsymbol{\tau})] + \mathbb{E}_{q^*}[\log q(\mathbf{a})] + \mathbb{E}_{q^*}[\log q(\tau_a)] \end{aligned}$$

Therefore, we can write the ELBO as the summation of 7 terms:

$$\text{ELBO}(q) = \mathbb{E}_{q^*}[\log p(\mathbf{Y}|\mathbf{Z}, \boldsymbol{\phi}, \boldsymbol{\tau}, \mathbf{a})] + \text{diff}_{\mathbf{Z}} + \text{diff}_{\boldsymbol{\phi}} + \text{diff}_{\boldsymbol{\tau}} + \text{diff}_{\boldsymbol{\pi}} + \text{diff}_{\mathbf{a}} + \text{diff}_{\tau_a} \quad (45)$$

where,

$$\text{diff}_{\mathbf{Z}} = \mathbb{E}_{q^*}[\log p(\mathbf{Z}|\boldsymbol{\pi})] - \mathbb{E}_{q^*}[\log q(\mathbf{Z})].$$

Specifically,

$$\text{diff}_{\mathbf{Z}} \equiv \sum_{i=1}^N \sum_{k=1}^K p_{ik}^* \mathbb{E}_{q^*(\boldsymbol{\pi})}(\log \pi_k) - \sum_{i=1}^N \sum_{k=1}^K p_{ik}^* \log p_{ik}^*.$$

The other terms in (45) are calculated as follows:

$$\text{diff}_{\boldsymbol{\phi}} \equiv -\frac{1}{2} \sum_{k=1}^K v_k^0 \{\text{trace}(\boldsymbol{\Sigma}_k^*) + (\mathbf{m}_k^* - \mathbf{m}_k^0)^T (\mathbf{m}_k^* - \mathbf{m}_k^0)\} + \frac{1}{2} \sum_{k=1}^K \log |\boldsymbol{\Sigma}_k^*|,$$

$$\text{diff}_{\boldsymbol{\tau}} \equiv \sum_{k=1}^K \{(b^0 - 1) \mathbb{E}_{q^*(\tau_k)}(\log \tau_k) - r^0 \mathbb{E}_{q^*(\tau_k)}(\tau_k)\} - \sum_{k=1}^K \{A_k^* \log R_k^* + (A_k^* - 1) \mathbb{E}_{q^*(\tau_k)}(\log \tau_k)\},$$

$$\text{diff}_{\boldsymbol{\pi}} \equiv \sum_{k=1}^K (d_k^0 - d_k^*) \mathbb{E}_{q^*(\boldsymbol{\pi})}(\log \pi_k),$$

$$diff_{\mathbf{a}} = -\frac{1}{2}\mathbb{E}_{q^*(\tau_a)}\tau_a \sum_{i=1}^N \mathbb{E}_{q^*(a_i)}a_i^2 + \sum_{i=1}^N \log \sigma_{a_i}^*,$$

$$\begin{aligned} diff_{\tau_a} &= (\alpha^0 - 1)\mathbb{E}_{q^*(\tau_a)}(\log \tau_a) - \beta^0\mathbb{E}_{q^*(\tau_a)}\tau_a - \alpha^* \log \beta^* - (\alpha^* - 1)\mathbb{E}_{q^*(\tau_a)}(\log \tau_a) + \beta^*\mathbb{E}_{q^*(\tau_a)}\tau_a \\ &= (\alpha^0 - \alpha^*)\mathbb{E}_{q^*(\tau_a)}(\log \tau_a) - (\beta^0 - \beta^*)\mathbb{E}_{q^*(\tau_a)}\tau_a - \alpha^* \log \beta^* \end{aligned}$$

and

$$\mathbb{E}_{q^*}[\log p(\mathbf{Y}|\mathbf{Z}, \boldsymbol{\phi}, \boldsymbol{\tau}, \mathbf{a})] = \sum_{i=1}^N \sum_{k=1}^K p_{ik}^* \left\{ \frac{n}{2} \mathbb{E}_{q^*(\tau_k)}(\log \tau_k) - \frac{1}{2} \frac{A_k^*}{R_k^*} \mathbb{E}_{q^*(\boldsymbol{\phi}_k) \cdot q^*(a_i)} [(\mathbf{Y}_i - \mathbf{B}\boldsymbol{\phi}_k - a_i \mathbf{1}_n)^T (\mathbf{Y}_i - \mathbf{B}\boldsymbol{\phi}_k - a_i \mathbf{1}_n)] \right\}.$$

Algorithm 2: Clustering functional data via variational inference with random intercepts

Data: N original curves with n evaluation points; number of clusters K ; values of

hyperparameters: $\mathbf{d}^0, \mathbf{m}_k^0, k = 1, \dots, K, s^0, b^0, r^0, \alpha^0, \beta^0$; convergence threshold and maximum number of iterations

Result: VB estimated mean curves for each cluster and the cluster index for each original curve

```
1 Initialization: initialize  $R_k^*, \mu_a^*$  and  $\beta^*$  with arbitrary values (e.g.,  $R_k^* = r^0, \mu_a^* = 0, \beta^* = \beta^0$ ) and  
    $p_{ik}^*$  from k-means, and set  $c = 0$ ;  
2 while  $c < \text{maximum number of iterations and difference of ELBO} > \text{convergence threshold}$  do  
3    $\alpha^* = \alpha^0 + \frac{N}{2}$ ;  
4   repeat  
5      $c = c + 1$ ;  
6     update  $A_k^{*(c)}$  using  $p_{1k}^{*(c-1)}, \dots, p_{Nk}^{*(c-1)}$  with equation (30);  
7     update  $\Sigma_k^{*(c)}$  using  $A_k^{*(c)}, R_k^{*(c-1)}$  and  $p_{1k}^{*(c-1)}, \dots, p_{Nk}^{*(c-1)}$  with equations (28) and (37);  
8     update  $\mathbf{m}_k^{*(c)}$  using  $\Sigma_k^{*(c)}, A_k^{*(c)}, R_k^{*(c-1)}, \mu_a^{*(c-1)}$  and  $p_{1k}^{*(c-1)}, \dots, p_{Nk}^{*(c-1)}$  with equations (29)  
       and (37);  
9     update  $\sigma_{a_i}^{*2(c)}$  using  $A_k^{*(c)}, R_k^{*(c-1)}, \alpha^*, \beta^{*(c-1)}$  and  $p_{ik}^{*(c-1)}, \dots, p_{iK}^{*(c-1)}$  with equations (32),  
       (37) and (40) ;  
10    update  $\mu_{a_i}^{*(c)}$  using  $\sigma_{a_i}^{*2(c)}, A_k^{*(c)}, R_k^{*(c-1)}$  and  $p_{ik}^{*(c-1)}, \dots, p_{iK}^{*(c-1)}$  with equations (33) and (37);  
11    update  $R_k^{*(c)}$  using  $\mathbf{m}_k^{*(c)}, \Sigma_k^{*(c)}, \sigma_{a_i}^{*2(c)}, \mu_{a_i}^{*(c)}$  and  $p_{1k}^{*(c-1)}, \dots, p_{Nk}^{*(c-1)}$  with equations (31) and  
       (44);  
12    update  $\beta^{*(c)}$  using  $\sigma_{a_i}^{*2(c)}$  and  $\mu_{a_i}^{*(c)}$  with equations (34) and (42);  
13    update  $\mathbf{d}^{*(c)}$  using  $p_{1k}^{*(c-1)}, \dots, p_{Nk}^{*(c-1)}$  with equations (26) and (36);  
14    update  $p_{1k}^{*(c)}, \dots, p_{Nk}^{*(c)}$  using  $A_k^{*(c)}, R_k^{*(c)}, \mathbf{d}^{*(c)}, \sigma_{a_i}^{*2(c)}, \mu_{a_i}^{*(c)}, \mathbf{m}_k^{*(c)}$  and  $\Sigma_k^{*(c)}$  with equations  
       (27), (37), (38), (39) and (44);  
15    calculate the current ELBO,  $\text{ELBO}^{(c)}$  using equation (45) ;  
16    difference of ELBO =  $\text{ELBO}^{(c)} - \text{ELBO}^{(c-1)}$ ;  
17  until maximum iteration is achieved or the ELBO converges;  
18 end
```

4 Simulation study

In Sections 4.1 to 4.4, we investigate the performance of the model proposed in Section 2 under various simulation scenarios. For the extension proposed in Section 3, results for one simulation scenario are presented in Section 4.5 as an example.

4.1 Simulation scenarios

Our simulation study comprises six different scenarios, five of which have three clusters ($K = 3$) while the last scenario has four clusters ($K = 4$). For each simulation scenario, we generate 50 datasets and apply the proposed VB algorithm to each dataset, considering the number of basis functions to be six except for Scenario 5, which uses 12 basis functions. The ELBO convergence threshold is 0.01, with a maximum of 100 iterations. For comparison purposes, we also investigate the performance of the k-means algorithm applied to the raw curves. In addition, we use the clustering results of k-means to initialize R_k^* and p_{ik}^* in our VB algorithm.

Scenarios 1 and 2 are adopted from Zambom et al. (2019). Each dataset is generated from 3 possible clusters ($k = 1, 2, 3$) with $N = 50$ curves per cluster. For each curve, we assume there are $n = 100$ observed values across a grid of equally spaced points in the interval $[0, \pi/3]$.

Scenario 1, $K = 3$:

$$Y_{ik}(t_j) = a_i + b_k + c_k \sin(1.3t_j) + t_j^3 + \delta_{ij}; \quad i = 1, \dots, 50; \quad j = 1, \dots, 100; \quad k = 1, 2, 3,$$

where $Y_{ik}(t_j)$ denotes the value at point t_j of the i th curve from cluster k , $a_i \sim U(-1/4, 1/4)$, $\delta_{ij} \sim N(0, 0.4^2)$, $b_1 = 0.3$, $b_2 = 1$, $b_3 = 0.2$, $c_1 = 1/1.3$, $c_2 = 1/1.2$, and $c_3 = 1/4$.

Scenario 2, $K = 3$:

$$Y_{ik}(t_j) = a_i + b_k \exp(c_k t_j) - t_j^3 + \delta_{ij}; \quad i = 1, \dots, 50; \quad j = 1, \dots, 100; \quad k = 1, 2, 3,$$

where $Y_{ik}(t_j)$ denotes the value at point t_j of the i th curve from cluster k , $a_i \sim U(-1/4, 1/4)$, $\delta_{ij} \sim N(0, 0.3^2)$, $b_1 = 1/1.8$, $b_2 = 1/1.7$, $b_3 = 1/1.5$, $c_1 = 1.1$, $c_2 = 1.4$, and $c_3 = 1.5$.

In Scenarios 3 and 4, each dataset is also generated considering three clusters ($k = 1, 2, 3$) with 50 curves each. The mean curve of the functional data in each cluster is generated from a pre-specified

linear combination of B-spline basis functions. The number of basis functions is the same across clusters but the coefficients of the linear combination are different, one set per cluster (see Table 1). We apply the function *create.bspline.basis* in the R package *fda* to generate six B-spline basis functions of order 4, $B_l(\cdot)$, $l = 1, \dots, 6$, evaluated on equally spaced points, t_j , $j = 1, \dots, 100$, in the interval $[0, 1]$.

Scenarios 3 and 4, $K = 3$:

$$Y_{ik}(t_j) = \sum_{l=1}^6 B_l(t_j)\phi_{kl} + \delta_{ij}; \quad i = 1, \dots, 50; \quad j = 1, \dots, 100; \quad k = 1, 2, 3,$$

where $Y_{ik}(t_j)$ denotes the value at point t_j of the i th curve from cluster k and $\delta_{ij} \sim N(0, 0.4^2)$. Table 1 presents the vector of coefficients for each cluster k , $\phi_k = (\phi_{k1}, \dots, \phi_{k6})^T$, used in Scenarios 3 and 4. Figure 1 illustrates the true mean curves for the three clusters and their corresponding basis functions for Scenarios 3 and 4.

Table 1: Coefficient vectors of six B-spline basis functions for each cluster in Scenarios 3 and 4

	Scenario 3						Scenario 4					
ϕ_k	ϕ_{k1}	ϕ_{k2}	ϕ_{k3}	ϕ_{k4}	ϕ_{k5}	ϕ_{k6}	ϕ_{k1}	ϕ_{k2}	ϕ_{k3}	ϕ_{k4}	ϕ_{k5}	ϕ_{k6}
$k = 1$	1.5	1	1.8	2	1	1.5	1.5	1	1.6	1.8	1	1.5
$k = 2$	2.8	1.4	1.8	0.5	1.5	2.5	1.8	0.6	0.4	2.6	2.8	1.6
$k = 3$	0.4	0.6	2.4	2.6	0.1	0.4	1.2	1.8	2.2	0.8	0.6	1.8

Scenario 5 ($K = 3$) is based on one of the simulation scenarios used in Dias et al. (2009) in which the curves mimic the energy consumption of different types of consumers in Brazil. There are 50 curves per cluster and for each curve we generate 96 points based on equally spaced time points, t_j , $j = 1, \dots, 96$ in the interval $[0, 24]$ (corresponding to one observation every 15 minutes over a 24-hour period).

Scenario 5, $K = 3$:

$$Y_{i1}(t_j) = 0.1(0.4 + \exp(-(t_j - 6)^2/3) + 0.2 \exp(-(t_j - 12)^2/25) + 0.5 \exp(-(t_j - 19)^2/4)) + \delta_{ij}$$

$$Y_{i2}(t_j) = 0.1(0.2 + \exp(-(t_j - 5)^2/4) + 0.25 \exp(-(t_j - 18)^2/5)) + \delta_{ij}$$

$$Y_{i3}(t_j) = 0.1(0.2 + \exp(-(t_j - 3)^2/4) + 0.25 \exp(-(t_j - 16)^2/5)) + \delta_{ij}$$

where $Y_{ik}(t_j)$ denotes the value at time t_j of the i th curve from cluster k , $i = 1, \dots, 50$, $j = 1, \dots, 96$, $k = 1, 2, 3$, and $\delta_{ij} \sim N(0, 0.012^2)$.

Scenario 6 also corresponds to one of the simulation scenarios considered by Zambom et al. (2019), where there are $K = 4$ clusters with 50 curves each. Each curve has 100 observed values based on equally spaced points, t_j , $j = 1, \dots, 100$, in the interval $[0, \pi/3]$.

Scenario 6, $K = 4$:

$$Y_{ik}(t_j) = a_i + b_k - \sin(c_k \pi t_j) + t_j^3 + \delta_{ij}; \quad i = 1, \dots, 50; \quad j = 1, \dots, 100; \quad k = 1, 2, 3, 4,$$

where $Y_{ik}(t_j)$ denotes the value at point t_j of the i th curve from cluster k , $a_i \sim U(-1/3, 1/3)$, $\delta_{ij} \sim N(0, 0.4^2)$, $b_1 = 0.2$, $b_2 = 0.5$, $b_3 = 0.7$, $b_4 = 1.3$, $c_1 = 1.1$, $c_2 = 1.4$, $c_3 = 1.6$ and $c_4 = 1.8$.

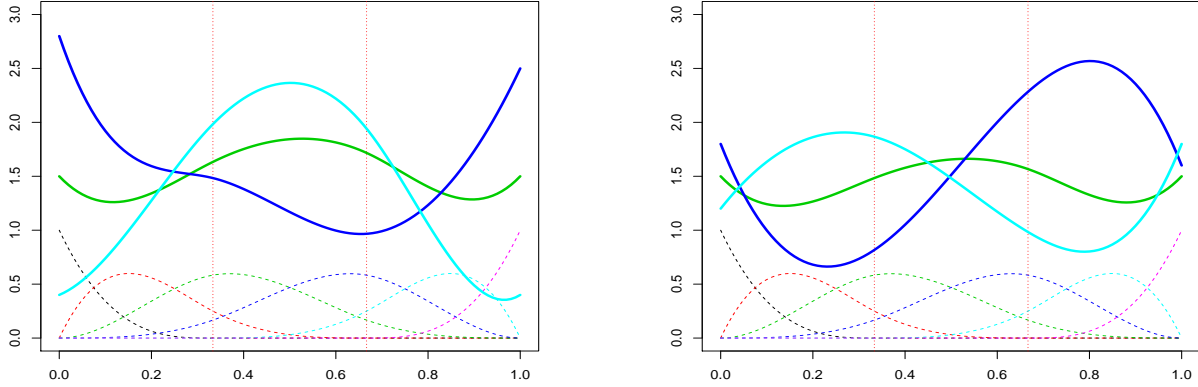


Figure 1: Cluster true mean curves (solid curves) and their corresponding six B-splines basis functions (dashed curves) for simulation scenarios 3 (left) and 4 (right).

4.2 Performance metrics

We evaluate the clustering performance of our proposed algorithm by two metrics: mismatches (Zambom et al., 2019) and V-measure (Rosenberg and Hirschberg, 2007). Mismatches are the proportion of subjects misclassified by the clustering procedure. In our case, each subject corresponds to a curve in our functional dataset. V-measure, a score between zero and one, evaluates the subject-to-cluster assignments and indicates the homogeneity and completeness of a clustering procedure result. Homogeneity

is satisfied if the clustering procedure assigns only those subjects that are members of a single group to a single cluster. Completeness is symmetrical to homogeneity, and it is satisfied if all those subjects that are members of a single group are assigned to a single cluster. The V-measure is one when all subjects are assigned to their correct groups in the clustering procedure.

In order to further evaluate the performance of the proposed VB algorithm in terms of the estimated mean curves, we calculate the empirical mean integrated squared error (EMISE) for each cluster in each simulation scenario. The EMISE is obtained as follows:

$$\text{EMISE}_k = \frac{T}{n} \sum_{j=1}^n \text{EMSE}_k(t_j), \quad (46)$$

where T is the evaluation interval length (e.g., $T = \pi/3$ in Scenario 1, Section 4.1), n is total number of observed evaluation points (e.g., $n = 100$ in Scenario 1), and the empirical mean squared error (EMSE) at point t_j for cluster k , $\text{EMSE}_k(t_j)$, can be calculated by

$$\text{EMSE}_k(t_j) = \frac{1}{S} \sum_{s=1}^S [f_k(t_j) - \hat{f}_k^s(t_j)]^2,$$

where s corresponds to the s th simulated dataset among S datasets in total, $f_k(t_j)$ is the value of the true mean function in cluster k evaluated at point t_j and $\hat{f}_k^s(t_j)$ is its corresponding estimated value for the s th simulated dataset. The estimated value $\hat{f}_k^s(t_j)$ is calculated using the B-spline basis expansion with coefficients corresponding to the posterior mean (13) obtained at the convergence of the VB algorithm.

4.3 Simulation results

Figure 2 shows the raw curves (colors differ from each cluster) from one of the 50 generated datasets for each simulation scenario. In addition, the true mean curves along with the estimated smoothed mean curves are shown in black and red, respectively. We can observe that the true and estimated mean curves almost coincide within each cluster in all scenarios.

Table 2 presents the mean and standard deviation of the mismatch rates and V-measure values over the 50 simulated datasets under each scenario for our proposed VB algorithm and k-means. Our VB algorithm performs better than k-means in Scenarios 1, 2, and 6, consisting of relatively parallel curves without crossing each other, but there are areas of overlap. In Scenarios 3 and 4, where we simulate data via a linear combination of six predefined basis functions, the proposed method has a better clustering performance than k-means, particularly in Scenario 3 with no mismatched curves, in contrast to a 17.15%

mismatch rate from k-means. These results are expected since, in these scenarios, the raw data are generated with the same structure as the proposed model. In Scenario 5, where we simulate data based on energy consumption, the VB algorithm also shows satisfactory performance, with only 2% of curves being misclassified compared to 10.53% for k-means.

Table 2: Mean mismatches rates and V-measure values for each simulation scenario.

Scenario	VB algorithm		k-means	
	M (sd)	V (sd)	M (sd)	V (sd)
1	0.0409 (0.0153)	0.8654 (0.035)	0.0488 (0.0181)	0.8594 (0.0388)
2	0.1416 (0.0334)	0.6300 (0.0655)	0.1739 (0.0517)	0.6188 (0.0650)
3	0.0000 (0.0000)	1.0000 (0.0000)	0.1715 (0.2312)	0.8738 (0.1700)
4	0.0000 (0.0000)	1.0000 (0.0000)	0.0559 (0.1531)	0.9581 (0.1145)
5	0.0200 (0.0800)	0.9840 (0.0639)	0.1053 (0.2005)	0.9227 (0.1469)
6	0.1054 (0.0197)	0.8043 (0.0262)	0.1398 (0.0655)	0.7819 (0.0546)

M: mean mismatches rate from 50 runs; V: mean V-measure from 50 runs;

sd: standard deviation.

In terms of V-measure, Table 2 shows that the proposed method resulted in average V-measure values above 0.8 in all scenarios except Scenario 2. V-measure mean values were higher for the proposed VB algorithm than k-means in all scenarios. We can observe that V-measure is more sensitive than mismatches rate, and a small increase in misclassification of the curves can make a marked drop in V-measure.

Table 3 presents the EMISE for each cluster in each Scenario. We can observe small EMISE values, which are consistent with the results shown in Figure 2, where there is a small difference between the red curves (i.e., the estimated mean functions) and the black curves (i.e., the true mean functions). A plot of EMSE values versus observed points for each cluster in Scenario 1 is presented in Figure 3. These plots also show higher EMSE values at the edges than at the middle of the evaluation interval.

4.4 Prior sensitivity analysis

In Bayesian analysis, it is important to assess the effects of different prior settings in the posterior estimation. In this section, we carry out a sensitivity analysis on how different prior settings may affect

Table 3: The empirical mean integrated squared error (EMISE) for the estimated mean curve in each cluster in each scenario.

Scenario	Cluster	EMISE	Scenario	Cluster	EMISE
1	1	0.00096	2	1	0.00164
	2	0.00077		2	0.00246
	3	0.00080		3	0.00169
3	1	0.00031	4	1	0.00023
	2	0.00045		2	0.00034
	3	0.00042		3	0.00033
5	1	0.00001	6	1	0.00076
	2	0.00114		2	0.00419
	3	0.00022		3	0.00472
				4	0.00130

the results of our proposed VB algorithm. Our sensitivity analysis focuses on the prior distribution of the coefficients ϕ_k of the B-spline basis expansion of each cluster-specific mean curve. We assume ϕ_k follows a multivariate normal prior distribution with a mean vector \mathbf{m}_k^0 and $s^0\mathbf{I}$ as the covariance matrix. We simulated data according to Scenario 3 and four different prior settings as follows:

- Setting 1: use the true coefficients as the prior mean vector and consider a small variance ($s^0 = 0.01$).
- Setting 2: use the true coefficients as the prior mean vector but consider a larger variance than in Setting 1 ($s^0 = 1$).
- Setting 3: use a prior mean vector that is different than the true vector of coefficients with a small variance ($s^0 = 0.01$).
- Setting 4: set the prior mean vector of coefficients to a vector of zeros with a small variance ($s^0 = 0.01$).

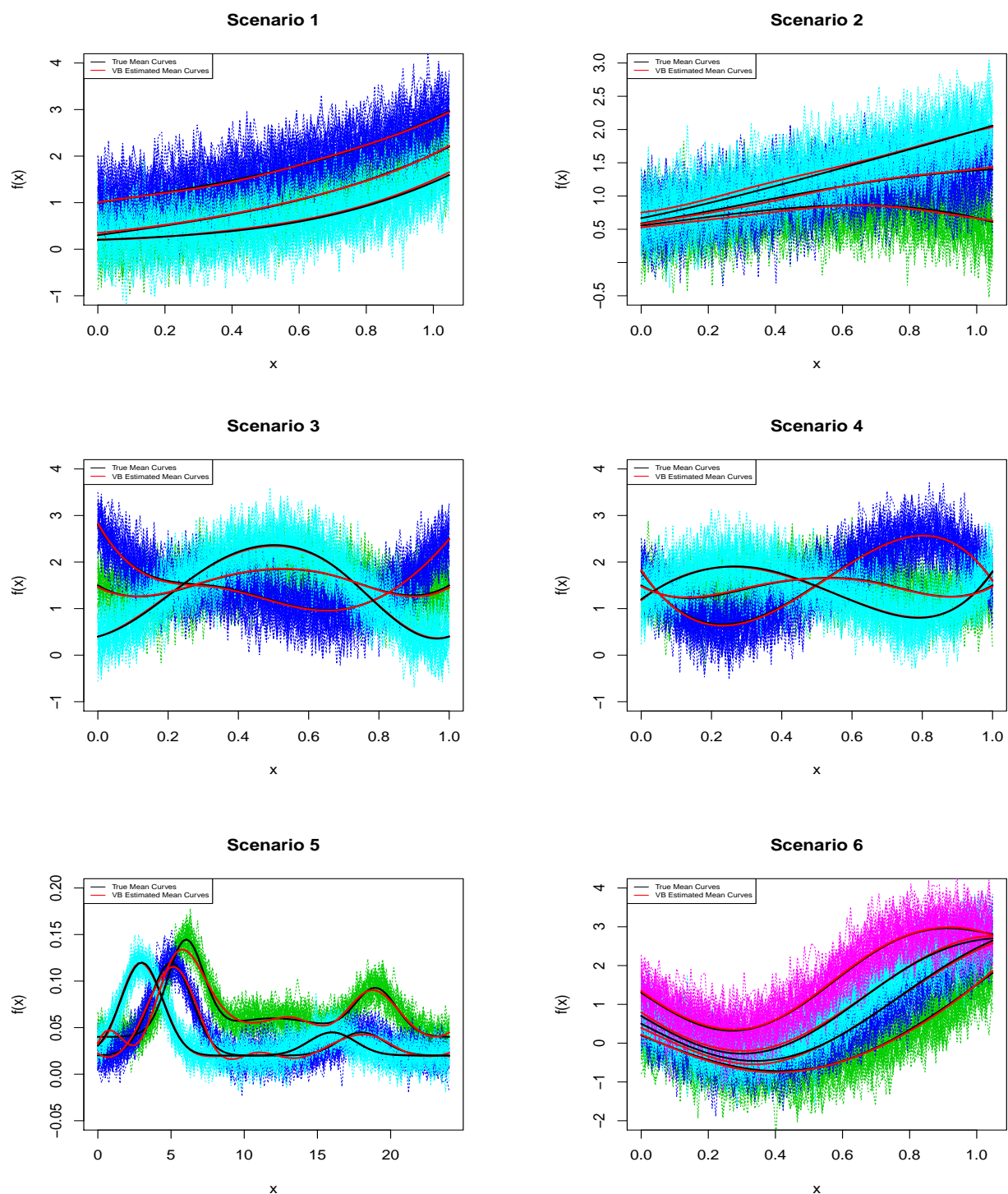


Figure 2: Example of simulated data under each proposed scenario. Raw curves (different colors correspond to different clusters), cluster-specific true mean curves (in black) and corresponding estimated mean curves (in red).

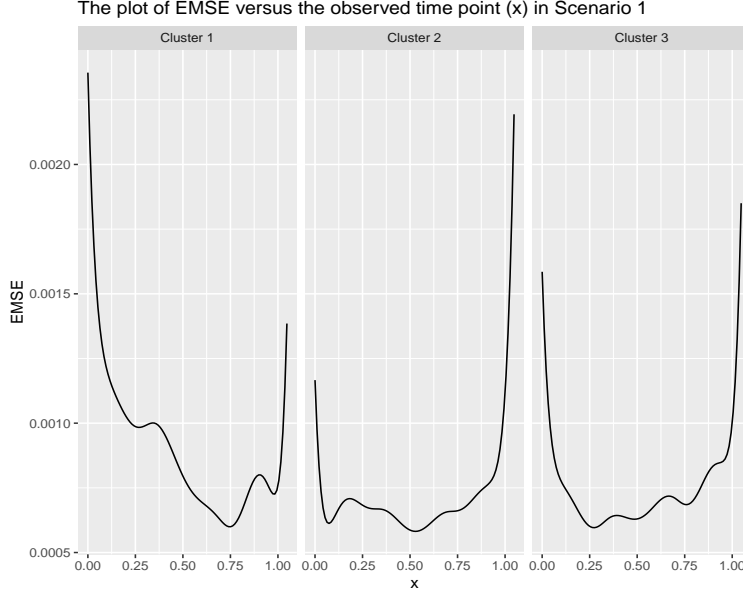


Figure 3: Empirical mean squared error (EMSE) versus each evaluation point x for each cluster in Scenario 1.

Setting 1 has the strongest prior information among these four prior settings, while setting 4 is the most non-informative prior case. In setting 3, the prior mean vector of coefficients is generated from sampling from a multivariate normal distribution with a mean vector corresponding to the true coefficients and covariance matrix $\sigma^2 \mathbf{I}$, with $\sigma^2 = 0.5$. For each prior setting, we simulate 50 datasets as in Scenario 3, obtaining the average mismatch rate and V-measure, which are displayed in Table 4. First, we can observe that all the curves are correctly clustered under Setting 1, which has the strongest prior information. Then, as we relax the prior assumptions in two possible directions (i.e., more considerable variance or less informative mean vector), the mismatch rate increases, and the V-measure decreases. However, the clustering performance does not decrease much, only 4.67% higher in mismatches and 3.73% lower in V-measure.

Table 4: Mean mismatches rates and V-measure values from prior sensitivity analysis in Scenario 3

Setting	1	2	3	4
M	0.0000	0.0067	0.0067	0.0467
V	1.0000	0.9947	0.9947	0.9627

M: mean mismatches rate from 50 runs; V: mean V-measure from 50 runs;

4.5 A simulation study on the extended model

We investigate the performance of the extended model with a random intercept using simulated data. We adopt the simulation scheme in Scenario 3 in Section 4.1, but add a random intercept to each curve. Therefore, in this scenario (called extended Scenario 3), data are generated as follows:

$$Y_{ik}(t_j) = a_i + \sum_{l=1}^6 B_l(t_j)\phi_{kl} + \delta_{ij}; \quad i = 1, \dots, 50; \quad j = 1, \dots, 100; \quad k = 1, 2, 3,$$

where $Y_{ik}(t_j)$ denotes the value at point t_j of the i th curve from cluster k , $a_i \sim N(0, 0.6^2)$ and $\delta_{ij} \sim N(0, 0.4^2)$. The B-spline coefficients, ϕ_{kl} , remain the same and are presented in Table 1.

We present the curves from one of the 50 simulated data sets in Figure 4. We can see a slight difference between each cluster's true mean curve and the estimated mean curve. Furthermore, more variation occurs after adding the random intercept. There is a more substantial overlap between the green and red curves, resulting in a more complex scenario for clustering than Scenario 3 in Section 4.1. Table 5 presents the numerical results, including the mean mismatch rate and the mean V-measure with their corresponding standard deviations from the 50 different runs. We can see that although both the standard deviations of mismatch rates and V-measures are larger than the ones obtained by k-means, our extended model provides a lower mean mismatches rate (lower by 13.31%) and a higher mean V-measure (higher by 23.04%). The larger standard deviation is because, among 50 different runs, there are 11 runs where our method can 100% correctly assign each curve to the cluster it belongs to, resulting in a mismatches rate of zero and a V-measure of one. At the same time, there is no run where k-means provides such perfect clustering results. Besides, among 50 different runs, there are 41 runs where our method provides lower mismatch rates and higher V-measures than k-means.

Table 5: Mean mismatches rates and V-measure values in the extended Scenario 3 using the extended model and compared with k-means

Scenario	VB algorithm		k-means	
	M (sd)	V (sd)	M (sd)	V (sd)
1	0.2493 (0.1416)	0.6078 (0.2285)	0.3824 (0.0367)	0.3774 (0.0581)

M: mean mismatches rate from 50 runs; V: mean V-measure from 50 runs;

sd: standard deviation.

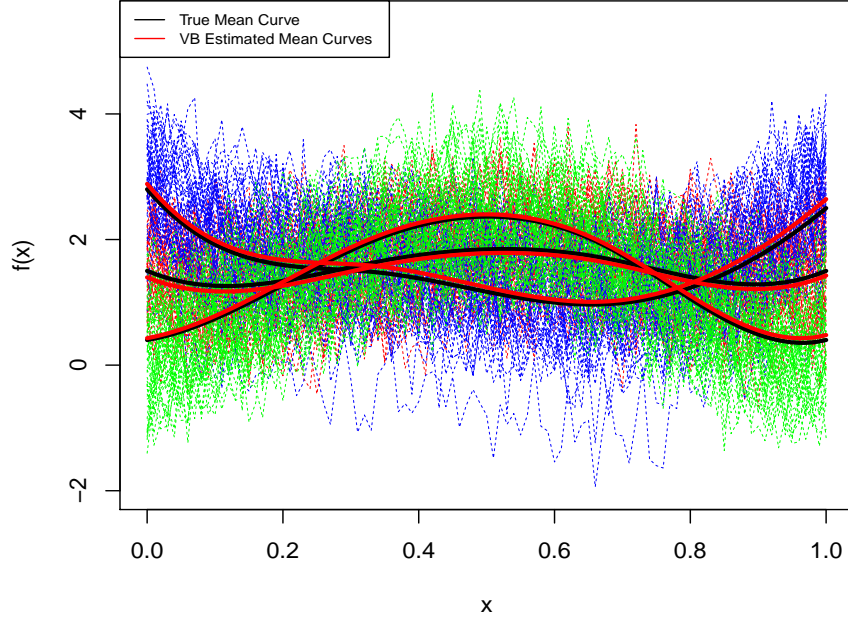


Figure 4: An example of simulated data using the extended model in the extended Scenario 3. Raw curves (different colors correspond to different clusters), cluster-specific true mean curves (in black) and corresponding estimated mean curves (in red).

5 Application to real data

In this section, we apply our proposed method in Section 2 to the growth and the Canadian weather datasets, which are both publicly available in the R package *fda*.

The Growth data (Tuddenham and Snyder, 1954) includes heights (in cm) of the 93 children over 31 unevenly spaced time points from the age of one to eighteen. Raw curves without any smoothing are shown in Figure 5, where the green curves correspond to boys and blue curves to girls. In this case, we apply our proposed method to the growth curves considering two clusters and compare the inferred cluster assignments (boys or girls) to the true ones.

The Canadian weather data (raw data are presented in Figure 8 in Appendix A) contains the daily temperature at 35 different weather stations (cities) in Canada, averaged out from the year of 1960 to 1994. However, unlike the growth data, we do not know the true number of clusters in the weather data. Therefore, in order to find the best number of clusters, we apply the deviance information criterion

(DIC) (Spiegelhalter et al., 2002) for model comparison. DIC is built to balance the model fitness and complexity under a Bayesian framework, and lower DIC indicates a better model. In our model setting, the DIC can be obtained as follows:

$$DIC = -4\mathbb{E}_{q^*}[\log p(\mathbf{Y}|\mathbf{Z}, \boldsymbol{\pi}, \boldsymbol{\phi}, \boldsymbol{\tau})] + 2\bar{D}, \quad (47)$$

where $\mathbb{E}_{q^*}[\log p(\mathbf{Y}|\mathbf{Z}, \boldsymbol{\pi}, \boldsymbol{\phi}, \boldsymbol{\tau})]$ can be computed after the convergence of our proposed VB algorithm based on the ELBO in (3). The term \bar{D} corresponds to the log-likelihood $\log p(\mathbf{Y}|\mathbf{Z}, \boldsymbol{\pi}, \boldsymbol{\phi}, \boldsymbol{\tau})$ evaluated at the expected value of each parameter posterior. For example, when we calculate the term $\log \tau_k$ in $\log p(\mathbf{Y}|\mathbf{Z}, \boldsymbol{\pi}, \boldsymbol{\phi}, \boldsymbol{\tau})$, we replace it by $\log [\mathbb{E}_{q^*(\tau_k)}(\tau_k)]$.

In our experiments, ten and six B-spline basis functions are considered for clustering the Growth and Canadian weather curves, respectively. The ELBO convergence threshold is 0.001. It is important to note that we do not have a strong prior knowledge of these real datasets but still need to provide appropriate priors for the VB algorithm. As a solution, we randomly select one underlying curve in each dataset and fit a B-spline regression to obtain a vector of coefficients which is then modified across different clusters resulting in the prior mean vectors \mathbf{m}_k^0 for $k = 1, \dots, K$. We set $s^0 = 0.1$ as the prior variance of these coefficients. For the Dirichlet prior distribution of $\boldsymbol{\pi}$, we use $\mathbf{d}^0 = (1/K, \dots, 1/K)$. For the Gamma prior distribution of the precision, $\tau_k = 1/\sigma_k^2$, we set $a^0 = 2000$ and $r^0 = 100$ for the growth data, and $a^0 = 1000$ and $r^0 = 800$ for the weather data.

Since we know there are two clusters (boys and girls) in the growth dataset, $K = 2$ is preset for the clustering procedure. We apply the proposed VB algorithm to cluster the growth curves with 50 runs corresponding to 50 different initializations. The classical k-means method is also applied to the raw curves for performance comparison purposes. Figure 5 presents the estimated mean curves for each cluster corresponding to the the best VB run (the one with maximum ELBO after convergence) along with the empirical mean curves. The empirical mean curves are calculated by considering the true clusters and calculating their corresponding point-wise mean at each time point. Some difference between the estimated and the empirical curves can be observed for the girls due to a potential outlier. Regarding clustering performance, the mismatch rates for the VB algorithm and k-means are 33.33% and 34.41%, respectively. V-measure is more sensitive to misclassification than mismatch rate and, therefore, we obtain low V-measure values of 7.75% for VB and 6.37% for k-means.

In the Canadian weather dataset, temperature data from stations located in Vancouver and Victoria were removed before modelling because they present relatively flat temperature curves compared to

other areas, meaning that they can be considered potential outliers. The right plot in Figure 6 shows the DIC values for different possible numbers of clusters ($K = 2, 3, 4, 5$). We can observe that the best number of clusters for separating the Canadian weather data is three, which corresponds to the smallest DIC. Finally, we present the clustering results with $K = 3$ on a map of Canada in the right plot in Figure 6. As can be seen, when $K = 3$, we have three resulted groups in three different colors. In general, those weather stations in purple are located in northern Canada. In contrast, those stations in southern Canada are separated into two groups: the West (in blue) and those in the East (in red). Although some stations may be wrongly clustered, we can still see a potential pattern that makes sense geographically. Combined with the information from DIC, three clusters should be adequate for clustering the Canadian weather data.

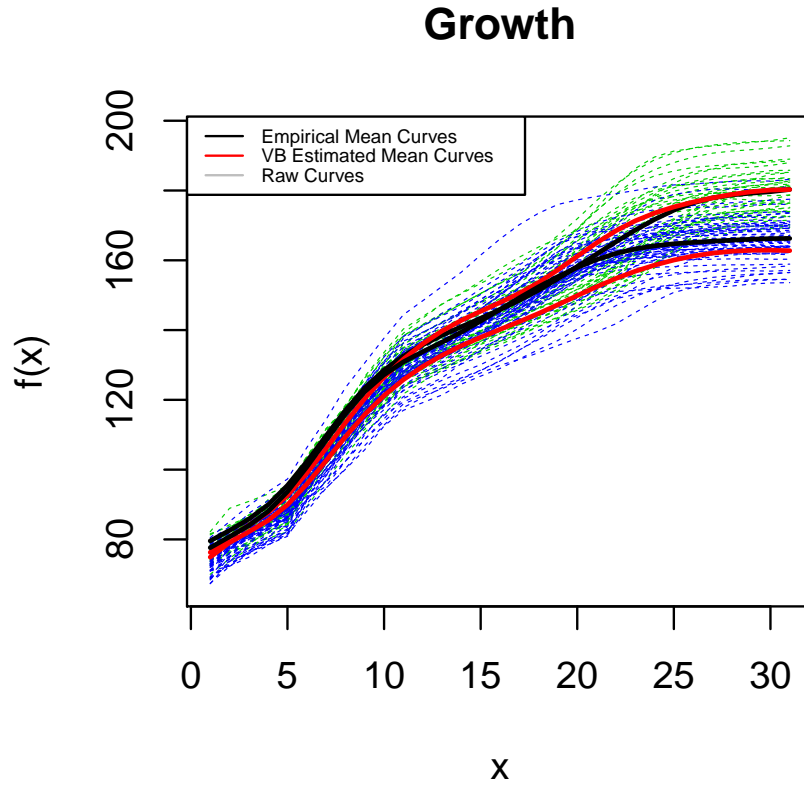


Figure 5: Raw curves (dashed curves) from the Growth dataset where green curves refer to the boys' heights while the blue ones are for the girls', with empirical mean curves (in solid black) and our VB estimated mean curves (in solid red).

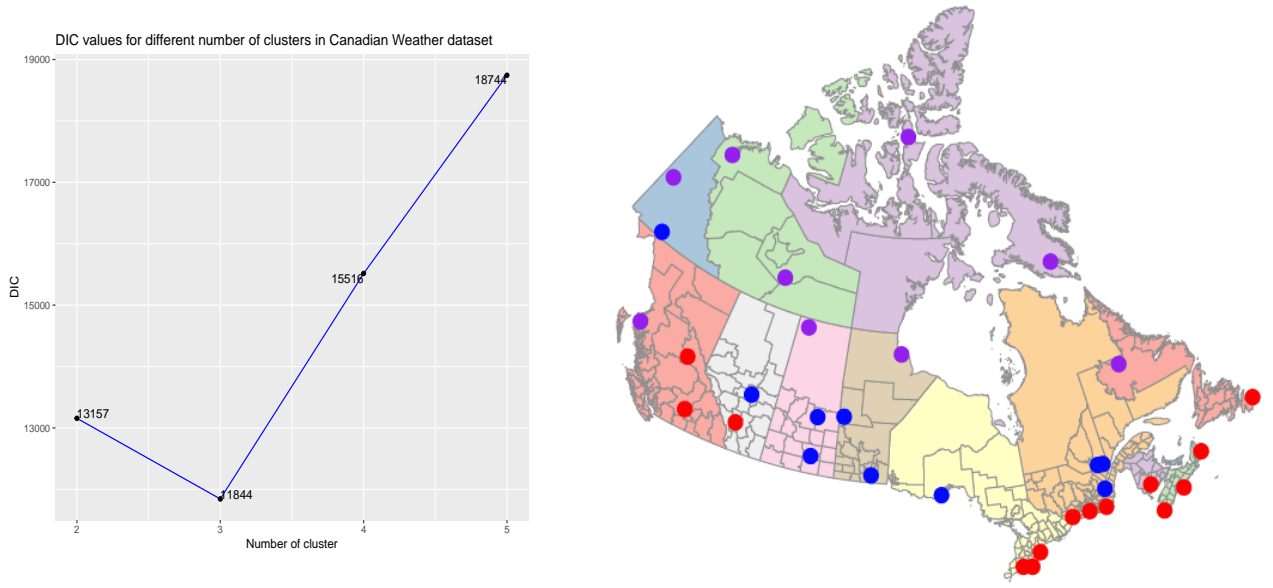


Figure 6: Left: DIC values for different clusters ($K = 2, 3, 4, 5$) in Canadian weather data. The best number of clusters is three which has the smallest DIC. Right: Clustering results (cities with same color are predicted in the same cluster) for Canadian weather data with preset three clusters ($K = 3$).

6 Conclusion and Discussion

This paper develops a new model-based algorithm to cluster functional data via Bayesian variational inference. We first provide an overview of variational inference, a method used to approximate the posterior distribution under the Bayesian framework through optimization. We then derive a mean-field Variational Bayes (VB) algorithm. Next, the coordinate ascent variational inference (CAVI) is applied to update each term in the variational distribution factorization until convergence of the evidence lower bound. Finally, each observed curve is assigned to the cluster with the largest posterior probability.

Simulations and real data analysis suggest that the proposed VB algorithm performs better than the classical k-means method in functional data with different patterns. In simulation studies, we also carried out a sensitivity analysis to show that our proposed VB algorithm still has a satisfactory performance across different prior settings. If we know the exact number of groups for real data, a fixed value can be set for K (e.g., $K = 2$ in the growth data) before running the algorithm. For cases where we do not know the exact number of clusters, the deviance information criterion (DIC) is adopted to guide the selection

of the best number of clusters.

The main advantage of our proposed VB algorithm is that we model the raw data and obtain clustering assignments and cluster-specific smooth mean curves simultaneously. In other words, compared to some previous methods where researchers first smooth the data and then cluster the data using only the information after smoothing (e.g., the coefficients of B-spline basis functions), our method directly uses the raw data as input, performing smoothing and clustering simultaneously. In addition, we can measure the uncertainty of our proposed clustering using the obtained cluster assignment posterior probabilities.

In the proposed model in Section 2, we assume the errors are independent, which may be a strong assumption. To make a more flexible version of VB algorithm, we extend our approach to include more complex variance-covariance structures by adding a random intercept for each curve. In the future work, we will carry out more numerical experiments to investigate the performance of the extended model.

References

- Bishop, C. (2006). *Pattern Recognition and Machine Learning*. Springer.
- Blei, D. M., Kucukelbir, A., and McAuliffe, J. D. (2017). Variational Inference: A Review for Statisticians. *Journal of the American Statistical Association*, 112(518):859–877.
- Boschi, T., Di Iorio, J., Testa, L., Cremona, M. A., and Chiaromonte, F. (2021). Functional data analysis characterizes the shapes of the first covid-19 epidemic wave in italy. *Scientific Reports*, 11(1).
- Chamroukhi, F. (2016). Piecewise regression mixture for simultaneous functional data clustering and optimal segmentation. *Journal of Classification*, 33(3):374–411.
- De Souza, C. P., Heckman, N. E., and Xu, F. (2017). Switching nonparametric regression models for multi-curve data. *Canadian Journal of Statistics*, 45(4):442–460.
- Delaigle, A., Hall, P., and Pham, T. (2019). Clustering functional data into groups by using projections. *Journal of the Royal Statistical Society: Series B (Statistical Methodology)*, 81(2):271–304.
- Dias, R., Garcia, N. L., Ludwig, G., and Saraiva, M. A. (2015). Aggregated functional data model for near-infrared spectroscopy calibration and prediction. *Journal of Applied Statistics*, 42(1):127–143.
- Dias, R., Garcia, N. L., and Martarelli, A. (2009). Non-parametric estimation for aggregated functional data for electric load monitoring. *Environmetrics*, 20:111 – 130.
- Franco, G., de Souza, C. P. E., and Garcia, N. L. (2021). Aggregated functional data model applied on clustering and disaggregation of uk electrical load profiles.
- Frizzarin, M., Bevilacqua, A., Dhariyal, B., Domijan, K., Ferraccioli, F., Hayes, E., Ifrim, G., Konkolewska, A., Nguyen, T. L., Mbaka, U., Ranzato, G., Singh, A., Stefanucci, M., and Casa, A. (2021). Mid infrared spectroscopy and milk quality traits: a data analysis competition at the ”international workshop on spectroscopy and chemometrics 2021”.
- Giacofci, M., Lambert-Lacroix, S., Marot, G., and Picard, F. (2013). Wavelet-based clustering for mixed-effects functional models in high dimension. *Biometrics*, 69(1):31–40.

- Hael, M. A., Yongsheng, Y., and Saleh, B. I. (2020). Visualization of rainfall data using functional data analysis. *SN Applied Sciences*, 2(3):461.
- Hartigan, J. and Wong, M. (1979). A k-means clustering algorithm. *J R Stat Soc Ser C*, 28:100–108.
- Hu, G., Geng, J., Xue, Y., and Sang, H. (2021). Bayesian spatial homogeneity pursuit of functional data: an application to the u.s. income distribution.
- Jacques, J. and Preda, C. (2013). Funclust: A curves clustering method using functional random variables density approximation. *Neurocomputing*, 112:164–171. Advances in artificial neural networks, machine learning, and computational intelligence.
- Jacques, J. and Preda, C. (2014). Functional data clustering: a survey. *Advances in Data Analysis and Classification*, 8(3):24.
- James, G. and Sugar, C. (2003). Clustering for sparsely sampled functional data. *Journal of the American Statistical Association*, 98(462):397–408.
- Jones, M. C. and Rice, J. A. (1992). Displaying the Important Features of Large Collections of Similar Curves. *The American Statistician*, 46(2):140.
- Jordan, M. I., Ghahramani, Z., Jaakkola, T., and Saul, L. (1999). Introduction to Variational Methods for Graphical Models. *Machine Learning*, 37:183–233.
- Kullback, S. and Leibler, R. A. (1951). On Information and Sufficiency. *The Annals of Mathematical Statistics*, 22(1):79 – 86.
- Lenzi, A., de Souza, C. P., Dias, R., Garcia, N. L., and Heckman, N. E. (2017). Analysis of aggregated functional data from mixed populations with application to energy consumption. *Environmetrics*, 28(2):e2414. e2414 env.2414.
- Li, T. and Ma, J. (2020). Functional data clustering analysis via the learning of gaussian processes with wasserstein distance. In Yang, H., Pasupa, K., Leung, A. C.-S., Kwok, J. T., Chan, J. H., and King, I., editors, *Neural Information Processing*, pages 393–403, Cham. Springer International Publishing.

- Martino, A., Ghiglietti, A., Ieva, F., and Paganoni, A. M. (2019). A k-means procedure based on a mahalanobis type distance for clustering multivariate functional data. *Statistical Methods & Applications*, 28(2):301–322.
- Ramsay, J., Hooker, G., and Graves, S. (2009). *Functional data analysis with R and MATLAB*. Springer New York.
- Ramsay, J. O. and Dalzell, C. J. (1991). Some tools for functional data analysis. *Journal of the Royal Statistical Society. Series B (Methodological)*, 53(3):539–572.
- Ramsay, J. O. and Silverman, B. W. (2005). *Functional Data Analysis*. Springer, 2 edition.
- Ray, S. and Mallick, B. (2006). Functional clustering by bayesian wavelet methods. *Journal of the Royal Statistical Society: Series B (Statistical Methodology)*, 68(2):305–332.
- Rosenberg, A. and Hirschberg, J. (2007). V-measure: A conditional entropy-based external cluster evaluation measure. In *Proceedings of the 2007 Joint Conference on Empirical Methods in Natural Language Processing and Computational Natural Language Learning (EMNLP-CoNLL)*, pages 410–420, Prague, Czech Republic. Association for Computational Linguistics.
- Samé, A., Chamroukhi, F., Govaert, G., and Aknin, P. (2011). Model-based clustering and segmentation of time series with changes in regime. *Advances in Data Analysis and Classification*, 5(4):301–321.
- Spiegelhalter, D. J., Best, N. G., Carlin, B. P., and Van Der Linde, A. (2002). Bayesian measures of model complexity and fit. *Journal of the Royal Statistical Society: Series B (Statistical Methodology)*, 64(4):583–639.
- Tarpey, T. and Kinader, K. (2003). Clustering functional data. *Journal of Classification*, 20(1):93–114.
- Tuddenham, R. D. and Snyder, M. M. (1954). Physical growth of california boys and girls from birth to eighteen years. *Publications in child development. University of California, Berkeley*, 1 2:183–364.
- Wainwright, M. J., Jordan, M. I., et al. (2008). Graphical models, exponential families, and variational inference. *Foundations and Trends® in Machine Learning*, 1(1–2):1–305.
- Wang, J.-L., Chiou, J.-M., and Müller, H.-G. (2016). Functional data analysis. *Annual Review of Statistics and Its Application*, 3:257–295.

- Ward, J. (1963). Hierarchical grouping to optimize an objective function. *J Am Stat Assoc*, 58:236–244.
- Yang, Y., Yang, Y., and Shang, H. L. (2021). Feature extraction for functional time series: Theory and application to nir spectroscopy data.
- Zambom, A., Collazos, J., and Dias, R. (2019). Functional data clustering via hypothesis testing k-means. *Computational Statistics*, 34(2):527–549.

A Plots

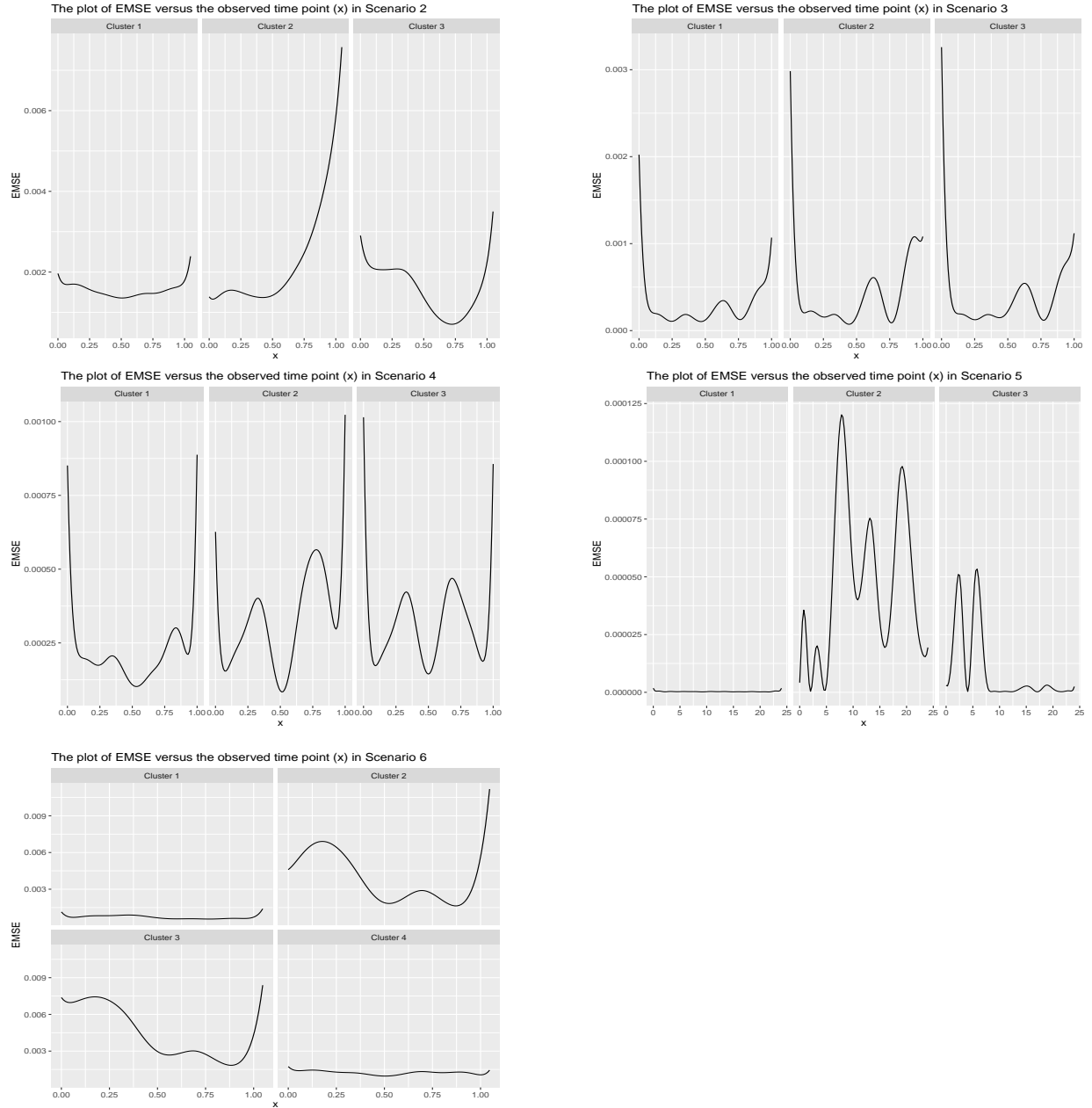


Figure 7: EMSE versus the observed evaluation point for each cluster in Scenarios 2, 3, 4, 5 and 6. In Scenario 5, the straight line in cluster one does not mean there is no EMSE. This is because compared to cluster two and three, the EMSE in cluster one is very small (the median is 1.41×10^{-11}).

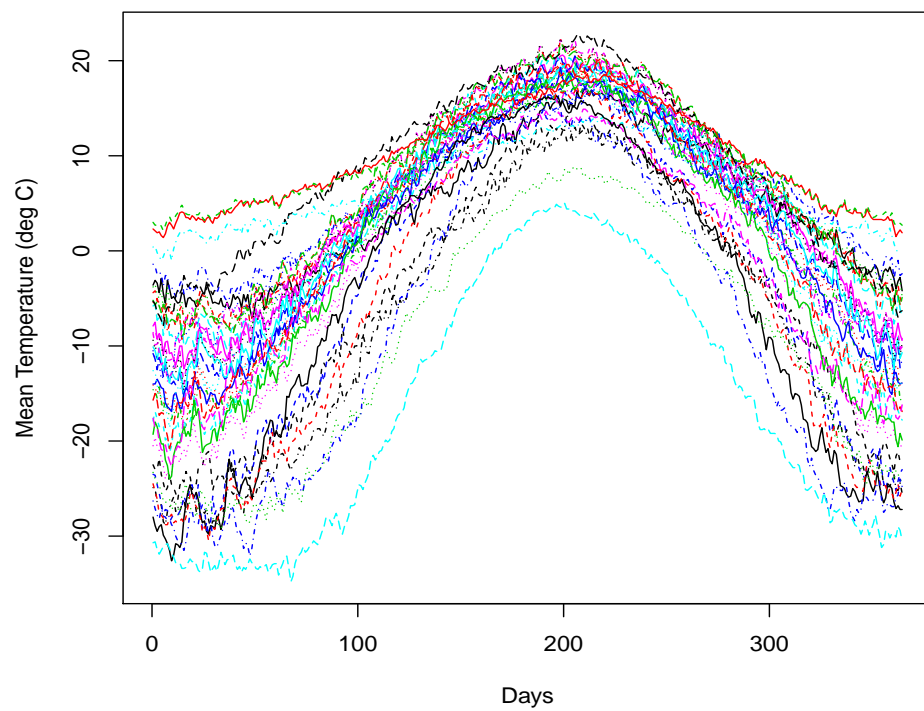


Figure 8: Raw curves of the Canadian weather data.